NASA Technical Memorandum 78805

A REVIEW AND ASSESSMENT OF THE STRESS-INTENSITY FACTORS FOR SURFACE CRACKS

J. C. Newman, Jr.

November 1978

NASA
National Aeronautics and Space Administration

Langley Research Center
Hampton, Virginia 23665

A REVIEW AND ASSESSMENT OF THE STRESS-INTENSITY FACTORS FOR SURFACE CRACKS

J. C. Newman, Jr.
NASA Langley Research Center
Hampton, VA 23665

ABSTRACT

The stress-intensity factor solutions proposed for a surface crack in a finite plate subjected to uniform tension are reviewed. Fourteen different solutions for the stress-intensity factors are compared. These solutions have been obtained over the past 16 years using approximate analytical methods, experimental methods, and engineering estimates.

The present paper assesses the accuracy of the various solutions by correlating fracture data on surface-cracked tension specimens made of a brittle epoxy material. Fracture of the epoxy material was characterized by a constant value of stress-intensity factor at failure. Thus, the correctness of the various solutions are judged by the variations in the stress-intensity factors at failure. The solutions were ranked in order of minimum standard deviation. The highest ranking solutions correlated 95 percent of data analyzed within ±10 percent, whereas the lowest ranking solutions correlated 95 percent of data analyzed within ±20 percent. However, some solutions could be applied to all data considered, whereas others were limited with respect to crack shapes and crack sizes that could be analyzed.

INTRODUCTION

Surface cracks [1,2] are among the most common flaws in many practical structures. Accurate stress-intensity factors for surface cracks are needed for reliable prediction of crack-growth rates and fractures strengths. Exact solutions are not available, but solutions have been obtained by approximate methods. However, due to the difficulties involved, these approximate solutions differ considerably.

In 1973, Merkle [3] and Keays [4] presented reviews of some of the earlier stress-intensity factor solutions for the surface crack. Since these reviews, the number of proposed solutions have nearly doubled. The objective of the present paper was to review the stress-intensity factor solutions proposed for the surface crack in a finite plate subjected to uniform tension and to assess the accuracy of the various solutions by correlating fracture data on a brittle material. Fourteen stress-intensity factor solutions were reviewed. Other solutions, those that had severe limitations on crack shape and crack size, were not considered in the assessment. This review was limited to linear-elastic analyses and to application to brittle materials.

The present assessment of the fourteen solutions was based on correlating fracture data. Fracture data from a large number of tests on surface-cracked tension specimens made of a brittle epoxy material were available in the literature [5]. In these data, the crack-depth-to-specimen-thickness ratios ranged from 0.15 to 1 and the crack-depth-to-crack-length ratios ranged from 0.3 to 0.84. Fracture of the epoxy material was characterized in the present paper by a constant value of stress-intensity factor at failure. Thus, the

correctness of the various solutions was judged by the variations in the stress-intensity factors at failure, and the solutions were ranked in order of minimum standard deviation. The range of applicability of the various solutions was also considered in assessing their usefulness.

SYMBOLS

a	depth of surface crack, m
c	half-length of surface crack, m
F	boundary-correction factor on stress intensity
K	mode I elastic stress-intensity factor, $N/m^{3/2}$
K_{cr}	fracture toughness, $N/m^{3/2}$
$M_e, M_k, M_s, M_t, M_1, M_2$	magnification factors defined in text
n	number of data analyzed
Q	elastic shape factor for an elliptical crack
S	gross-section stress, N/m^2
t	specimen thickness, m
W	specimen width, m
σ	standard deviation
Φ	complete elliptic integral of second kind
ϕ	parametric angle of ellipse

ELASTIC STRESS-INTENSITY FACTORS

The stress-intensity factor solutions for cracks in finite plates are usually expressed in terms of a boundary-correction factor that modifies the stress-intensity factor for cracks in infinite bodies. Thus, the elastic solution for an elliptical crack embedded in an infinite solid (Fig. 1) has a major role in the surface-crack solution. In this section, a brief review of the stress-intensity factors for the elliptical crack embedded in an infinite solid and the form of stress-intensity factor for the surface crack in a finite plate are presented.

Infinite Solid

Irwin [1] derived an exact expression for the mode I stress-intensity factor around an elliptical crack in an infinite elastic solid subjected to uniform tension (Fig. 1) based on an exact stress analysis by Green and Sneddon [6]. The stress-intensity factor along the boundary of the elliptical crack was given by

$$K = \frac{S\sqrt{\pi a}}{\Phi}\left(\frac{a^2}{c^2}\cos^2\phi + \sin^2\phi\right)^{1/4} \tag{1}$$

where Φ is the complete elliptic integral of second kind and is given by

$$\Phi = \int_0^{\pi/2} \left(\sin^2\phi + \frac{a^2}{c^2}\cos^2\phi\right)^{1/2} d\phi \tag{2}$$

As is customary, the elliptic integral is expressed in terms of the elastic shape factor, Q. The shape factor Q equals Φ^2.

Very useful empirical expressions for Q have been developed by Rawe (see Ref. 3). The expressions are

$$\left.\begin{aligned} Q &= 1 + 1.464\left(\frac{a}{c}\right)^{1.65} \quad \text{for} \quad \frac{a}{c} \leq 1 \\ Q &= 1 + 1.464\left(\frac{c}{a}\right)^{1.65} \quad \text{for} \quad \frac{a}{c} > 1 \end{aligned}\right\} \tag{3}$$

The maximum error in the stress-intensity factor by using these equations for Q was about 0.13 percent for all values of a/c. (Rawe's original equation was written in terms of $a/2c$.)

For $c > a$ the maximum stress-intensity factor is at $\phi = \pi/2$ and is given by

$$K = S\sqrt{\pi \frac{a}{Q}} \tag{4}$$

Finite Plate

The surface crack in a finite plate is shown in Figure 2. The crack is semi-elliptical with a crack of half-length c and of depth a. The plate is of thickness t and width, W, which is usually large with respect to the crack length. The configuration is subjected to a uniform tensile stress, S, normal to the crack plane. The form of the mode I stress-intensity factor is given by

$$K = S\sqrt{\pi \frac{a}{Q}}\, F\left(\frac{a}{t}, \frac{a}{c}, \frac{c}{W}, \phi\right) \tag{5}$$

The boundary-correction factor, F, accounts for the influence of the front face, back face, and finite width on the stress-intensity factor for a crack in an infinite solid. The parametric angle is defined in the insert on Figure 2. Many analysts, through approximation techniques, have tried to determine the correct

expression for F. Some of the approximate methods used were the alternating method, finite-element method, boundary-integral equations, method of lines, line-spring model, experimental methods, and engineering estimates.

In the Appendix, fourteen solutions [1,7-22] for the boundary-correction factor, F, are presented. Table I gives the chronological order of development for these solutions, the method used, limitations on a/c, a/t and 2c/W, and the form of the results. The solutions were given in either graphical or equation form. Most solutions were proposed for analyzing fracture of surface-cracked tension specimens and give the stress-intensity factor at the maximum depth point. A few give the stress-intensity factors at other locations along the crack front for a/c ratios greater than about 0.6. Some solutions also included plasticity corrections for analyzing fracture of ductile materials. However, in the present paper only the elastic solutions are presented and used.

COMPARISON OF STRESS INTENSITY CORRECTION FACTORS

Figures 3 to 6 show a comparison among the various stress intensity correction factors for the surface crack subjected to uniform tension for some common crack shapes (a/c) as a function of a/t. Figure 3 shows the stress intensity correction factor, F, at the maximum depth point ($\phi = \pi/2$) for a crack with an a/c ratio of 0.2. The stress-intensity factor at the maximum depth point was also the maximum stress-intensity value. The solid and dashed curves show correction factors obtained from equations and graphs, respectively. These results show that for a/t

ratios less than about 0.2, most solutions were in good agreement (± 5 percent). However, for a/t ratios greater than 0.2, the differences among the various solutions were considerable. The percentage differences were as large as 80 percent for an a/t ratio of 0.6. The upper solid line at $a/t = 1$ ($F = 2.35$) denotes the equivalent correction factor for a through crack of length $2c$ in an infinite plate. This is the approximate limiting value for the surface crack as a/t approaches unity.

Figure 4 shows the correction factor at the maximum-depth point but for a crack with an a/c ratio of 0.6. The stress-intensity factor at $\phi = \pi/2$ was also the maximum stress intensity for most solutions which reported the variation in stress intensity along the crack front [3, 18 and 22]. In Reference 22, for an a/t ratio of 0.8 the maximum stress intensity did not occur at the maximum depth point but occurred near the intersection of the crack with the front face ($\phi=0$). Figure 4 shows that for a/t ratios less than about 0.3, most solutions agree within about 5 percent. For an a/t ratio of 0.6, the percentage difference between the upper and lower bounds was about 20 percent. Again, the upper solid line at $a/t = 1$ ($F = 1.65$) denotes the approximate limiting value for the surface crack as a/t approaches unity.

Figures 5 and 6 show the correction factor at $\phi = \pi/2$ and the maximum value, respectively, for a semi-circular surface crack ($a/c = 1$). The maximum stress-intensity factor occurred at or near the intersection of the crack with the front surface, $\phi = 0$. Some of the fourteen solutions reviewed were not included in these figures because they did not consider the semi-circular crack or their results should not be applied

to these particular values of ϕ. Figure 5 shows that all solutions, except the estimate from Irwin [1], agree within about 5 percent for a/t ratios less than 0.4. For larger a/t ratios, the percentage difference was as large as 35 percent. The results from Hellen and Blackburn [26] (not included in the fourteen solutions reviewed) have also been included in Figure 5 for comparison. Hellen and Blackburn analyzed only the semi-circular surface crack using a three-dimensional finite-element analysis.

Figure 6 shows the maximum stress-intensity factors for semi-circular surface cracks as calculated by four investigators. The maximum stress-intensity values reported in the literature [3, 21, and 26], occurred at or near the intersection of the crack with the front face. Again, the finite-element results from Hellen and Blackburn [26] and unpublished results from Kobayashi have also been included for comparison. The results from Kobayashi were obtained using the analysis described in Reference 20. For a/t ratios less than 0.3, the solutions were in good agreement. However, for larger a/t ratios, the solutions generally disagree (as much as 30 percent). The results from Kobayashi and Raju and Newman [21] were in good agreement (within 5 percent).

Some of the differences shown in Figures 3 to 6 may be attributed to improper boundary conditions imposed on the surface-crack configuration. Some of the earlier stress-intensity factor solutions [10, 17] did not analyze the surface-crack configuration, but analyzed approximate configurations for which solutions could be readily obtained, such as an elliptical crack approaching a free boundary in a semi-infinite solid [18] or two elliptical cracks approaching each other in an infinite solid. Kobayashi [20] has also demonstrated that his earlier applications of the

alternating method inadvertently induced improper bending restraint by limiting the areas of front- and back-faces that are free of residual surface tractions. The more recent analyses of the surface crack [21, 25 and 26] have used the finite-element method and any inaccuracies in these analyses would be associated with modeling the surface crack and with how well the governing equations in the interior were satisfied.

ANALYSIS OF FRACTURE DATA

The accuracy of the stress-intensity factor solutions, previously reviewed, were independently verified herein by analyzing fracture data from the literature on brittle epoxy materials. These data had a wide range in crack shape (a/c) and crack size (a/t). Solutions which gave the best correlation of data and which applied over the widest range of a/c and a/t were regarded as the most useful.

Smith [5] conducted fracture tests on a large number of surface-crack tension specimens made of a brittle epoxy material (ultimate tensile strength of about 60 MPa). All his specimens were 25 mm wide and had thicknesses ranging from 2.5 to 9.5 mm. He conducted 150 fracture tests on specimens with a/t ratios that ranged from 0.15 to 1 and a/c ratios that ranged from 0.3 to 0.84. The test specimens were arranged into five different groups. Each group of specimens was manufactured at a different time (denoted with a "plate date") and each group had the same specimen thickness. The estimated plane-strain plastic-zone size using the largest value of fracture toughness (computed) was about 0.015 mm. This estimated plastic-zone size was orders of magnitude smaller than the minimum specimen thickness. The extremely small plastic

zone indicates that linear-elastic analyses are adequate.

The fourteen stress-intensity factor solutions presented in the Appendix were used herein to analyze Smith's fracture data on epoxy specimens. Fracture was characterized herein by a constant value of stress-intensity factor at failure (denoted as K_{cr}). The fracture toughness, K_{cr}, for each group of specimens was calculated for each solution by averaging the stress-intensity factors at failure for data where the a/t ratios were less than 0.5 and was given by

$$K_{cr} = \frac{1}{n} \sum_{i=1}^{n} K_i \tag{6}$$

where n is the number of data analyzed for each group of specimens. This particular limit on a/t was chosen because, as previously mentioned, for low a/t ratios most solutions were in fair agreement. Thus, the calculated fracture toughness values would also be in fair agreement. The fracture toughness values computed from the various solutions for each group of specimens are given in Table II. As expected, the maximum and minimum K_{cr} values from the various solutions for each "plate date" material were in fair agreement (within ±10 percent of their average value).

ASSESSMENT OF THE SOLUTIONS

To assess the accuracy of the various stress-intensity factor solutions, comparisons are made between the calculated stress-intensity factors at failure and the fracture toughness, K_{cr}, for all fracture data considered ($0.15 \leq a/t \leq 1$; $0.3 \leq a/c \leq 0.84$). Thus, for a/t ratios greater than 0.5, these comparisons show how well the various solutions predict failure of the epoxy specimens. Fracture data which exceeded the limitations on a/t or a/c for each solution (see Table I) were not included in the analysis using that particular solution.

Figures 7 through 20 show the ratio of the stress-intensity factor at failure normalized by the fracture toughness, K_{cr}, plotted against the a/t ratio for each solution. The fracture toughness values used for each group of specimens are given in Table II. The solid line at unity denotes perfect agreement and the dashed lines denote ±10 percent scatter. Stress-intensity factor ratios (K/K_{cr}) that deviate substantially from unity indicate substantial deficiencies in that particular solution. (The ratio of K/K_{cr} is equivalent also to the ratio of experimental failure stress to predicted failure stress.) The standard deviation (σ) and the number of tests analyzed (n) are also shown on each figure.

To rank the various solutions, the standard deviation was calculated from the results for each stress-intensity factor solution. The standard deviation was given by

$$\sigma = \sqrt{\frac{\sum_{i=1}^{n} e_i^2}{n-1}} \tag{7}$$

where n is the number of data points analyzed and

$$e_i = \frac{K_i}{K_{cr}} - 1 \tag{8}$$

K_i is the stress-intensity factor at failure for each data point considered and K_{cr} is the fracture toughness for that particular group of specimens.

The ranking of the various solutions in order of minimum standard deviation is shown in Table III. This table shows the investigator(s),

date of publication, limitation on a/t, percent of data analyzed, standard deviation and the form of the results for each solution. The standard deviations ranged from .044 to .089 for the fourteen solutions considered. Assuming a normal distribution, two standard deviations ($\pm 2\sigma$) about the mean ($K/K_{cr} = 1$) form bounds in which 95 percent of the data should fall. The highest ranking solutions correlated 95 percent of the data analyzed within ± 10 percent, whereas the lowest ranking solutions correlated 95 percent of the data analyzed within ±20 percent. However, the percent of data analyzed ranged from 57 to 100 percent. Of the lowest ranking solutions, most underestimated the stress-intensity factors for a/t ratios greater than 0.5 (K/K_{cr} less than unity); and one solution (Newman, Fig. 15) overestimated the stress-intensity factors for a/t greater than about 0.8.

The stress-intensity factor solutions which gave low values of standard deviation tended to give large values for the correction factors shown in Figures 3 to 5. Those solutions which used stress-intensity factors at locations other than the maximum-depth point for the near semi-circular cracks (Figs. 9, 19, and 20), generally, gave low values of standard deviation. Only three solutions (Fig. 15, 19 and 20) used a finite-width correction on the stress-intensity factor for the surface crack. Analyses made with a finite-width correction gave slightly lower values of standard deviation than did the same analyses made without a width correction (see Table III, Raju and Newman, 1977).

CONCLUDING REMARKS

The stress-intensity factor solutions proposed for a surface crack in a finite plate subjected to uniform tension were reviewed. These solutions have been developed over the past sixteen years using approximate analytical methods, experimental methods, and engineering estimates. Comparison of the various solutions at the maximum depth point showed good agreement ($\pm$5 percent) for crack-depth-to-specimen-thickness ratios less than about 0.3. However, for larger crack-depth-to-specimen-thickness ratios (0.3 to 1) the solutions were in considerable disagreement (20 to 80 percent), especially, for cracks with small crack-depth-to-crack-length ratios (0.2 to 0.6). Some of the discrepancies among the various solutions were attributed to improper boundary conditions imposed on the surface-crack configuration.

To assess the accuracy of the various solutions, fracture data on surface-crack tension specimens made of a brittle epoxy material were analyzed. The various solutions were ranked on the variation in the stress-intensity factors at failure. Standard deviations ranged from .044 to .089 for the fourteen stress-intensity factor solutions considered. The solutions, ranked in order of minimum standard deviation, were Raju-Newman, Smith, Newman-Raju, Paris-Sih, Masters-Haese-Finger, Irwin, Newman, Kobayashi, Smith-Alavi, Rice-Levy, Smith-Sorensen, Shah-Kobayashi, Anderson-Holmes-Orange, and Kobayashi-Moss. The highest ranking solutions correlated 95 percent of the data analyzed within $\pm$10 percent, whereas the lowest ranking solutions correlated 95 percent of data analyzed within $\pm$20 percent. However, some solutions were applied to all data considered, whereas others were limited on crack shapes and crack sizes that could be analyzed.

APPENDIX

BOUNDARY-CORRECTION FACTORS FOR SURFACE CRACKS IN FINITE PLATES

The fourteen expressions for the boundary-correction factor, F, used in the text are briefly reviewed herein. The stress-intensity factor is given by equation 5.

Irwin (1962)[1]. - He estimated the boundary-correction factor for a shallow semi-elliptical surface crack in a finite-thickness plate at $\phi = \pi/2$ as

$$F = \sqrt{1.2} \approx 1.1 \tag{9}$$

The coefficient 1.1 accounted for the combined influence of both the front- and back-face effects in the range $0 \leq a/t \leq 0.5$ and $0 \leq a/c \leq 1$.

Paris and Sih (1965)[7] - They estimated the correction factor at $\phi = \pi/2$, which included a front- and back-face correction, as

$$F = \left[1 + 0.12\left(1 - \frac{a}{c}\right)\right]\sqrt{\frac{2t}{\pi a}\tan\left(\frac{\pi a}{2t}\right)} \tag{10}$$

for $a/t \leq 0.75$ and $a/c \leq 1$. The "tangent" term was obtained from an analysis of an infinite plate (two dimensional) containing an infinite periodic array of cracks.

Smith (1966)[3,8]. - He proposed a modification of the semi-circular surface crack solution, given in Reference 8, to obtain an estimate for a semi-elliptical surface crack in a finite-thickness plate under tension

(Boeing Airplane Co., Structural Development Research Memorandum No. 17, Aug. 1966, see Ref. 3). The solution presented in Reference 8, using the alternating method, was the first analysis to consider the variation of stress intensity around the crack front for a semi-circular surface crack in a semi-infinite solid.

For fracture, he proposed to use the maximum stress-intensity factor for which the correction factor was given by

$$F = M_1 M_2 f(\theta) \tag{11}$$

where M_1 and M_2 are the front- and back-face magnification factors, respectively, and $f(\theta)$ is an angular function [8] ($\theta = \pi/2 - \phi$). The maximum value of the product M_1 times $f(\theta)$ for various a/c ratios is

a/c	$M_1 f(\theta)$
.2	1.09
.4	1.075
.6	1.06
.8	1.07
1.0	1.21

The back-face magnification factor, M_2, for $a/c = 1$ was obtained by Smith using the alternating method (see Ref. 3). Using M_2 for $a/c = 1$ and the single edge-crack solution for $a/c = 0$ [9], curves of M_2 for other a/c ratios were estimated by graphical interpolation. The curves for M_2 have been reproduced in Reference 3 on page 25. These curves had various limitations on the maximum a/t ratio. For $a/c = 0.2$, the

maximum a/t ratio was less than 0.6 and for $a/c = 1$, the maximum a/t ratio was less than about 0.9.

Kobayashi and Moss (1969)[10]. - They estimated the correction factor as

$$F = M_1 M_2 \tag{12}$$

where M_1, the front-face magnification factor, was given by

$$M_1 = 1 + 0.12 \left(1 - \frac{a}{c}\right)^2 \tag{13}$$

The back-face magnification factor, M_2, was obtained from an existing solution for a pair of coplanar elliptical cracks under uniform tension, with a plane of symmetry (simulated back face) located midway between the two cracks [10]. Assuming no interaction between the front- and back-faces, boundary-correction factors were estimated for ratios of a/c ranging from 0 to 1 and ratios of a/t ranging from 0 to 0.98. The curves for the correction factors (product of M_1 and M_2) are given in Reference 10 (page 42).

Masters, Haese, and Finger (1969)[11]. - They used an experimental method to obtain the correction factors. The experimental method involved fracture tests of surface-crack tension specimens (with various a/c and a/t ratios) made of 2219-T87 aluminum alloy material ($t = 16$mm) at room and cryogenic temperature. The correction factors were then obtained by requiring that the calculated stress-intensity factor be equal to the plane-strain fracture toughness, K_{Ic}, at the same test temperature. The correction factors were given as

$$F = 1.1\, M_K \tag{14}$$

for $a/t < 0.85$ and $0.1 \leq a/c \leq 0.8$. The curves for M_K are given in Reference 11 (page 67 , Fig. 58). These same correction factors have also been used to correlate fracture data on aluminum and titanium alloys in Reference 12.

Smith and Alavi (1969)[13]. - They were the first to analyze the part-circular surface crack in a semi-infinite solid using the alternating method. The crack was a segment of a circle where the crack depth, a, was less than the crack length, c. The boundary-correction factor for the part-circular surface crack in a finite-thickness plate was given by

$$F = M_s M_t \tag{15}$$

for $a/t \leq 0.8$ and $0.4 \leq a/c \leq 1$. M_s was the front-face magnification and M_t was the back-face magnification. M_s was the same as the product of M_1 times $f(\theta)$ in equation (11). The back-face magnification was estimated from the solution for an embedded circular crack near a free boundary in a semi-infinite solid. Curves of M_t for various a/c ratios are given in Reference 3 (page 33).

Rice and Levy (1970)[14]. - They determined the stress-intensity factors at $\phi = \pi/2$ using a "line spring" model. The line spring model reduces the three-dimensional crack problem to a two-dimensional analogy (single-edge-cracked plate) where the crack is represented as a line of reduced stiffness. The results of their analysis were presented graphically in terms of the ratio of the stress-intensity factor at the

deepest point of a semi-elliptical surface crack (K_I) to the stress-intensity factor for a single-edge-cracked specimen (K_∞) with a crack of the same depth. The correction factor, rewritten in terms of equation 5, was given by

$$F = \left(\frac{K_I}{K_\infty}\right)\sqrt{Q}\ f \tag{16}$$

where K_I/K_∞ was obtained from Reference 14 for uniform tension and f, the correction factor for a single-edge-cracked plate [9], was given by

$$f = 1.12 - 0.23\ (\frac{a}{t}) + 10.55\ (\frac{a}{t})^2 - 21.71\ (\frac{a}{t})^3 + 30.38\ (\frac{a}{t})^4 \tag{17}$$

They calculated the ratio of K_I/K_∞ for $0.1 \leq \frac{a}{t} \leq 0.7$ and $0 \leq \frac{a}{c} \leq 1$.

Anderson, Holms, and Orange (1970)[15]. - They modified the boundary-correction factor equation of Paris and Sih [7] and estimated the correction factor as

$$F = \left[1 + 0.12\ (1 - \frac{a}{c})\right]\sqrt{\frac{2tQ}{\pi a}\tan\ (\frac{\pi a}{2tQ})} \tag{18}$$

for $a/t \leq 1$ and $\frac{a}{c} \leq 1$ where Q is the elastic shape factor.

Newman (1972)[16]. - He used the analytical results from Smith and Alavi [12], Rice and Levy [13], and Gross and Srawley [9] for particular ranges of a/c to obtain an expression for the correction factor. The results from Smith and Alavi for a near semi-circular crack (a/c = 0.4 and 1), Rice and Levy for shallow cracks (a/c = 0.1 and 0.2), and Gross

and Srawley for a single-edge crack (a/c = 0) were used. An equation was chosen to fit these particular results. The equation for the correction factor was given by

$$F = M_e = \left[M_1 + \left(\sqrt{Q \frac{c}{a}} - M_1 \right) \left(\frac{a}{t} \right)^p \right] \sqrt{\sec \left[\frac{\pi c}{W} \frac{a}{t} \right]} \tag{19}$$

where

$$p = 2 + 8 \left(\frac{a}{c} \right)^3 \tag{20}$$

The expression for Q was approximated by

$$\left.\begin{aligned} Q &= 1 + 1.47 \left(\frac{a}{c} \right)^{1.64} \quad \text{for} \quad \frac{a}{c} \leq 1 \\ Q &= 1 + 1.47 \left(\frac{c}{a} \right)^{1.64} \quad \text{for} \quad \frac{a}{c} > 1 \end{aligned}\right\} \tag{21}$$

The maximum error in the stress-intensity factor by using three equations for Q was about 0.25 percent. The front-face correction, M_1, was given by

$$\left.\begin{aligned} M_1 &= 1.13 - 0.1 \left(\frac{a}{c} \right) \quad \text{for} \quad 0.02 \leq \frac{a}{c} \leq 1 \\ M_1 &= \sqrt{\frac{c}{a}} \left(1 + 0.03 \frac{c}{a} \right) \quad \text{for} \quad \frac{a}{c} > 1 \end{aligned}\right\} \tag{22}$$

For $\frac{a}{c} < .02$, the stress-intensity factor for the single-edge cracked plate (a/c = 0) subjected to uniform tension [9] was assumed to apply and F was given by equation 17.

As a/t approaches unity for any value of a/c (except zero), equation 5 with F given by equation 19 reduces to the stress-intensity factor for a through crack of length 2c in a finite-width plate. The "secant" term in equation 19 is the finite-width correction.

Shah and Kobayashi (1972)[17]. - They estimated the correction factors from an empirical front-face magnification (M_1) and from an analytical back-face magnification (M_2) obtained from the solution for an embedded elliptical crack approaching the free surface of a semi-infinite solid [18]. The front-face magnification was given by equation 13. The correction factor, due to both the front- and back-faces, was obtained by multiplying the back-face magnification, M_2, by equation 13. The correction factor was given by

$$F = M_K = M_1 M_2 \tag{23}$$

for $a/t \leq 0.9$ and $0.1 \leq \frac{a}{c} \leq 1$. The curves for M_K are given in Reference 17 (page 114).

Smith and Sorensen (1974)[19]. - They used the alternating method to calculate the variation of the stress-intensity factor along semi-elliptical surface cracks in finite-thickness plates. They made calculations for a/c ratios ranging from 0.1 to 0.6. The results for a/c ratios of 0.8 and 1 used by Smith and Sorensen were obtained from Shah and Kobayashi [17]. The boundary-correction factors are presented in Reference 19 (page 88).

Kobayashi (1976)[20]. - He used the alternating method with improved boundary conditions to obtain the correction factors. In previous analyses by Kobayashi using the alternating method some inappropriate boundary

conditions (bending restraints) were inadvertently induced by limiting the areas of front- and back-face surfaces that are free of residual surface tractions. To estimate the effect of this bending restraint, a two-dimensional finite-element model of a single-edge-cracked tension plate was analyzed with side constraints. The side constraints induced a similar bending moment. The change in stress intensity caused by this bending moment was calculated and used to modify the stress intensity for the surface crack. The stress-intensity factors at the maximum depth point were calculated for $a/c = 0.2$ and 0.98. The stress-intensity factor for other a/c ratios (0.4, 0.6 and 0.8) were obtained by interpolation between the results from $a/c = 0.2$ and 0.98. The correction factors were given by $F = M_K$ for $a/t \leq 0.9$ and $0.2 \leq a/c \leq 0.98$. The curves for M_K are given in Reference 20 (Fig. 12).

Raju and Newman (1977)[21,22]. - They used a three-dimensional finite-element analysis with singularity elements to obtain the correction factors. To verify the accuracy of the finite-element method, elliptical cracks ($a/c = 0.2$ to 1) embedded in a large solid body were analyzed [21] and the stress-intensity factors agreed generally within 1 percent of the exact solutions [6]. To verify the finite-element models employed, convergence was studied by varying the number of degrees of freedom from 1500 to 6900. The correction factors were calculated for semi-elliptical surface cracks ($a/c = 0.2$ to 2) in finite-thickness plates with a/t ranging from 0.2 to 0.8 for $W \geq 10c$. The correction factors are tabulated in References 21 and 22.

For fracture, they proposed to use the maximum stress-intensity factor for $a/c < 0.6$. For a/c ratios between 0.6 and 1, an "average"

stress-intensity factor (average between the values at $\phi = 0$ and $\phi = \pi/2$) was used. These results were calculated for a surface crack in a wide plate. To compensate for the influence of finite width, the results were multiplied by f_w, the finite-width correction [23] given by

$$f_w = \sqrt{\sec\left[\frac{\pi c}{W}\sqrt{\frac{a}{t}}\right]} \tag{24}$$

Newman and Raju (1978) . - They used the results from Raju and Newman [21,22] for the semi-elliptical surface crack and from Gross and Srawley [9] for a single-edge crack to obtain an equation for the correction factors. The form of the equation was similar to that used in Reference 16. The equation was given by

$$F = M_e = \left[M_1 + \left(\sqrt{Q\,\frac{c}{a}} - M_1\right)\left(\frac{a}{t}\right)^p + \sqrt{Q\,\frac{c}{a}}\,(M_2 - 1)\left(\frac{a}{t}\right)^{2p}\right] f_w \tag{25}$$

where $p = \sqrt{\pi}$ and Q is given by equations 3. The front-face correction, M_1, was given by

$$\left.\begin{aligned} M_1 &= 1.13 - 0.1\left(\frac{a}{c}\right) \quad \text{for} \quad .03 \le \frac{a}{c} \le 1 \\ M_1 &= \sqrt{\frac{c}{a}}\left(1 + .03\,\frac{c}{a}\right) \quad \text{for} \quad \frac{a}{c} > 1 \end{aligned}\right\} \tag{26}$$

and M_2 was given by

$$\left.\begin{aligned} M_2 &= \sqrt{\frac{\pi}{4}} \quad \text{for} \quad \frac{a}{c} \le 1 \\ M_2 &= 1 + \frac{c}{a}\left(\sqrt{\frac{\pi}{4}} - 1\right) \quad \text{for} \quad \frac{a}{c} > 1 \end{aligned}\right\} \tag{27}$$

The finite-width correction, f_w, was given by equation 24. For $\frac{a}{c} < .03$, the stress-intensity factor for the single-edge crack plate, $a/c = 0$, subjected to uniform tension [9] was assumed to apply and F was given by equation 17.

Other Analyses of the Surface Crack. - A large number of reports consider the surface-crack configuration. Some of these reports analyze [24-27] or experimentally determine [28] the stress-intensity factors for only a few select configurations. The results from these reports were too limited in values of a/c and a/t to use in the "Analysis of Fracture Data" section. Many other reports (see, for example, References [29-30]) use stress-intensity factor solutions previously reviewed. One report [31] analyzes the surface-crack configuration from a non-fracture mechanics approach.

REFERENCES

[1] Irwin, G. R., The Crack Extension Force for a Part Through Crack in a Plate, ASME, J. Appl. Mechs., Vol. 29, No. 4, 1962, pp. 651-654.

[2] The Surface Crack: Physical Problems and Computational Solutions, The American Society of Mechanical Engineers, ed. J. L. Swedlow, 1972.

[3] Merkle, J. G., A Review of Some of the Existing Stress Intensity Factor Solutions for Part-Through Surface Crack, Oak Ridge National Laboratory, ORNL-TM-3983, Jan. 1973.

[4] Keays, R. H., A Review of Stress Intensity Factors for Surface and Internal Cracks, Australia Aero. Res. Lab., Report ARL/SM 343, April 1973.

[5] Smith, F. W., The Elastic Analysis of the Part-Circular Surface Flaw Problem by the Alternating Method, The Surface Crack: Physical Problems and Computational Solutions, ed. J. L. Swedlow, 1972, pp. 125-152.

[6] Green, A. E. and Sneddon, I. N., The Distribution of Stress in the Neighborhood of a Flat Elliptical Crack in an Elastic Solid, Proc. Cambridge Phil. Soc., Vol. 46, 1950, pp. 159-164.

[7] Paris, P. C. and Sih, G. C., Stress Analysis of Cracks, ASTM STP-381, 1965, pp. 30-83.

[8] Smith, F. W., Emery, A. F., and Kobayashi, A. S., Stress Intensity Factors for Semi-Circular Cracks, Part 2 - Semi-Infinite Solid, J. Appl. Mechs., Vol. 34, No. 4, Trans. ASME, Vol. 89, Series E, Dec. 1967, pp. 953-959.

[9] Gross, B. and Srawley, J. E., Stress-Intensity Factors for Single-Edge Notch Specimens in Bending or Combined Bending and Tension by Boundary Collocation of a Stress Function, NASA TN D-2603, 1965.

[10] Kobayashi, A. S. and Moss, W. L., Stress Intensity Magnification Factors for Surface-Flawed Tension Plate and Notched Round Tension Bar, Fracture, Chapman and Hall, 1969, pp. 31-45.

[11] Masters, J. N., Haese, W. P., and Finger, R. W., Investigation of Deep Flaws in Thin Walled Tanks, NASA CR-72606, Dec. 1969.

[12] Masters, J. N., Bixler, W. D., and Finger, R. W., Fracture Characteristics of Structural Aerospace Alloys Containing Deep Surface Flaws, NASA CR-134587, Dec. 1973.

[13] Smith, F. W. and Alavi, M. J., Stress-Intensity Factors for a Part-Circular Surface Flaw, Proceedings of the First International Conference on Pressure Vessel Technology, Delft, The Netherlands, ASME, 1969, pp. 783-800.

[14] Rice, J. R. and Levy, N., The Part-Through Surface Crack in an Elastic Plate, Tech. Rept. NASA NGL 40-002-080/3, Div. of Engr. Brown University, Trans. ASME, J. Appl. Mech., Paper No. 71-APM-20 (1970).

[15] Anderson, R. B., Holmes, A. G., and Orange, T. W., Stress Intensity Magnification for Deep Surface Cracks in Sheets and Plates, NASA TN D-6054, Oct. 1970.

[16] Newman, J. C., Jr., Fracture Analysis of Surface- and Through-Cracked Sheets and Plates, Symposium on Fatigue and Fracture, George Washington Univ., 1972 (Also, Engr. Fracture Mechs., Vol. 5, 1973, pp. 667-689).

[17] Shah, R. C. and Kobayashi, A. S., On the Surface Flaw Problem, The Surface Crack: Physical Problems and Computational Solutions, ed. J. L. Swedlow, 1972, pp. 79-124.

[18] Shah, R. C. and Kobayashi, A. S., Stress-Intensity Factors for an Elliptical Crack Approaching the Surface of a Semi-Infinite Solid, Int. J. of Fracture, Vol. 9, No. 2, June 1973.

[19] Smith, F. W. and Sorensen, D. R., Mixed Mode Stress Intensity Factors for Semi-elliptical Surface Cracks, NASA CR-134684, 1974.

[20] Kobayashi, A. S., Crack-Opening Displacement in a Surface-Flawed Plate Subjected to Tension or Plate Bending, Proc. Second Int. Conf. on Mechanical Behavior of Materials, ASM, 1976, p. 1073.

[21] Raju, I. S. and Newman, J. C., Jr., Improved Stress-Intensity Factors for Semi-Elliptical Surface Cracks in Finite-Thickness Plates, NASA TMX-72825, Aug. 1977.

[22] Raju, I. S. and Newman, J. C., Jr., Stress-Intensity Factors for a Wide Range of Semi-Elliptical Surface Cracks in Finite-Thickness Plates, Engineering Fracture Mechanics Journal, 1979.

[23] Newman, J. C., Jr., Predicting Fracture of Specimens With Either Surface Cracks or Corner Cracks at Holes, NASA TN D-8244, June 1976.

[24] Miyamoto, H. and Miyoshi, T., Analysis of Stress Intensity Factor for Surface Flawed Tension Plate, Proc. Symposium on High Speed Computing of Elastic Structures, IUTAM, Liege, Aug. 1970.

[25] Atluri, S. and Kathiresan, A., An Assumed Displacement Hybrid Finite Element Model for Three-Dimensional Linear Fracture Mechanics Analysis, Proc. 12th Annual Meeting of the Soc. Engr. Science, Univ. of Texas, Austin, TX, Oct. 1975.

[26] Hellen, T. K. and Blackburn, W. S., The Calculation of Stress Intensity Factors in Two and Three Dimensions Using Finite Elements, Computational Fracture Mechanics, ASME, 1975, p. 103.

[27] Gyekenyesi, J. P. and Mendelson, A., Stress Analysis and Stress Intensity Factors for Finite Geometry Solids Containing Rectangular Surface Cracks, NASA TMX-71964, 1977.

[28] Harms, A. E. and Smith, C. W., Stress Intensity Factors for Long, Deep Surface Flaws in Plates Under Extensional Fields, NASA CR-132015, Feb. 1973.

[29] Orange, T. W., A Semiempirical Fracture Analysis for Small Surface Cracks, NASA TN D-5340, July 1969.

[30] Broek, D., Nederveen, A. and Meulman, A., Applicability of Fracture Toughness Data to Surface Flaws and to Corner Cracks at Holes, National Aerospace Laboratory, NLR TR 71033U, Jan. 1971.

[31] Kuhn, P., Residual Tensile Strength in the Presence of Through Cracks or Surface Cracks, NASA TN D-5432, March 1970.

TABLE I.- Stress-Intensity Factor Solutions for the Surface Crack in Chronological Order

Investigator(s)	Date	Ref	Method (a)	Limitations			Form of Results
				a/t	a/c	2c/W	
Irwin	1962	1	EE	≤ 0.5	0 to 1	(b)	Eq.
Paris-Sih	1965	7	EE	≤ 0.75	0 to 1	(b)	Eq.
Smith	1966	3,8	AM&EE	f(a/c)	.2 to 1	(b)	Graph
Kobayashi-Moss	1969	10	AM&EE	≤ 0.98	0 to 1	(b)	Graph
Masters-Haese-Finger	1969	11	EM	≤ 0.85	.1 to .8	(b)	Graph
Smith-Alavi	1969	13	AM&EE	≤ 0.8	.4 to 1	(b)	Graph
Rice-Levy	1970	14	LSM	≤ 0.7	0 to 1	(b)	Graph
Anderson-Holms-Orange	1970	15	EE	≤ 1.0	0 to 1	(b)	Eq.
Newman	1972	16	EE	≤ 1.0	.02 to ∞	< 1	Eq.
Shah-Kobayashi	1972	17	AM	≤ 0.9	.1 to 1	(b)	Graph
Smith-Sorensen	1974	19	AM	≤ 0.9	.1 to 1	(b)	Graph
Kobayashi	1976	20	AM&EE	≤ 0.9	.2 to 1	(b)	Graph
Raju-Newman	1977	21,22	FEM	≤ 0.8	.2 to 2	(b)	Graph
Newman-Raju	1978	---	FEM&EE	≤ 1.0	.03 to ∞	$< .5$	Eq.

(a) Engineering estimate (EE), Alternating method (AM), Line-spring model (LSM), Finite-element method (FEM)

(b) Effects of finite width were not considered.

TABLE II.- Fracture Toughness, K_{cr} ($kN/m^{3/2}$) for Brittle Epoxy Material Calculated from Various Stress-Intensity Factor Solutions

Investigator(s)	Plate date				
	8-7-69	10-6-70	12-5-70	4-11-71	6-10-71
Irwin	686	634	678	664	681
Paris-Sih	653	648	692	672	684
Smith	697	670	699	697	710
Kobayashi-Moss	654	609	658	652	670
Masters-Haese-Finger	699	663	712	696	704
Smith-Alavi	659	619	671	664	680
Rice-Levy	597	565	599	613	640
Anderson-Holmes-Orange	646	608	660	674	693
Newman	658	616	670	674	693
Shah-Kobayashi	653	610	659	653	671
Smith-Sorensen	638	604	652	652	670
Kobayashi	676	661	733	729	741
Raju-Newman	708	697	724	716	729
Newman-Raju	677	682	731	713	723

TABLE III.- Ranking of Stress-Intensity Factor Solutions for the Surface Crack in Order of Minimum Standard Deviation

Investigator(s)	Date	Ref	Limitation a/t	Percent of Data Analyzed	Standard Deviation	Form of Results
Raju-Newman	1977	21,22	0.8	90	.044 (a)	Graph
Smith	1966	3,8	f(a/c)	90	.045	Graph
Newman-Raju	1978	---	1.0	100	.048	Eq.
Paris-Sih	1965	7	0.75	86	.052	Eq.
Masters-Haese-Finger	1969	11	0.85	88	.055	Graph
Irwin	1962	1	0.5	57	.056	Eq.
Newman	1972	16	1.0	100	.060	Eq.
Kobayashi	1976	20	0.9	98	.060	Graph
Smith-Alavi	1969	13	0.8	84	.066	Graph
Rice-Levy	1970	14	0.7	79	.068	Graph
Smith-Sorensen	1974	19	0.9	98	.072	Graph
Shah-Kobayashi	1972	17	0.9	98	.077	Graph
Anderson-Holms-Orange	1970	15	1.0	100	.085	Eq.
Kobayashi-Moss	1969	10	0.98	99	.089	Graph

(a) Standard deviation without finite-width correction, f_w, was .048.

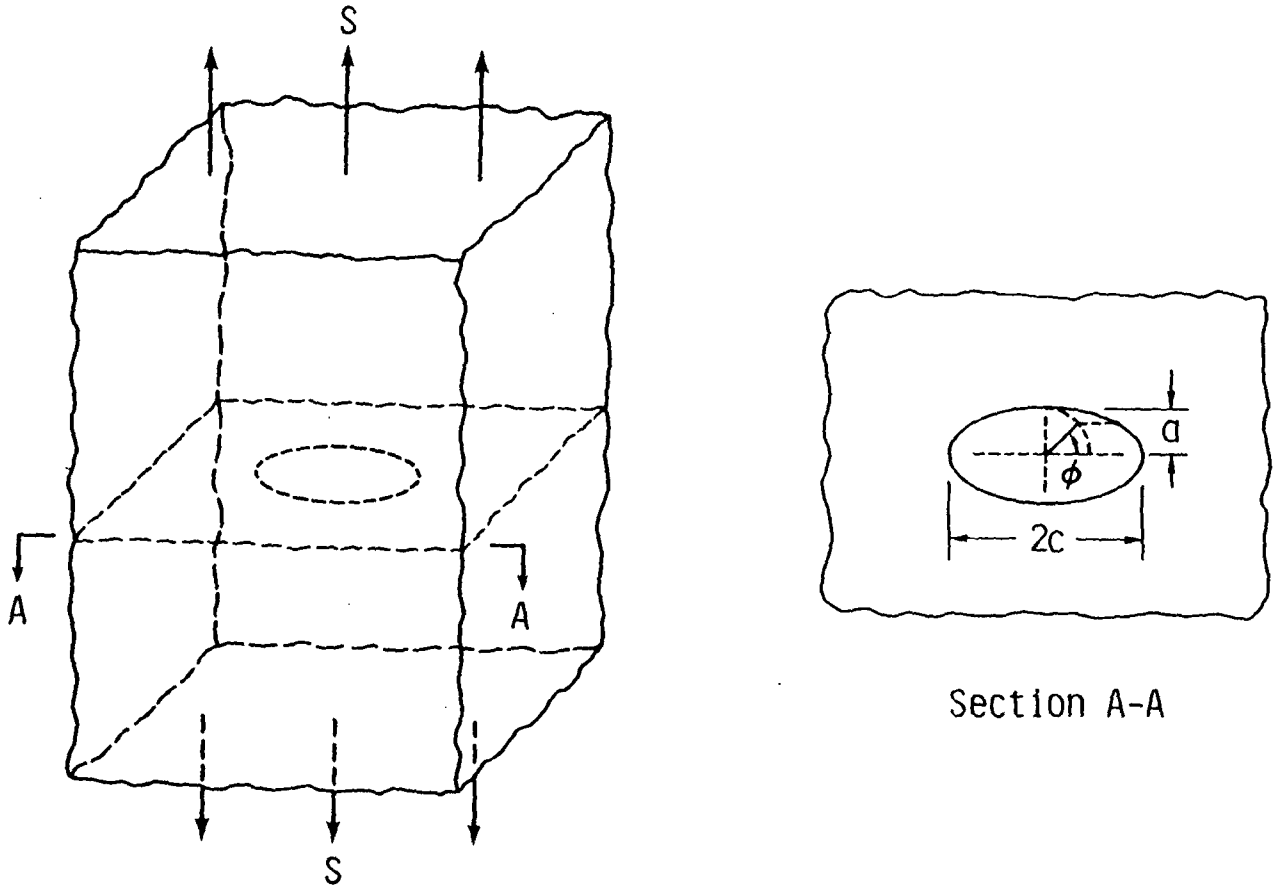

Fig. 1- Embedded elliptical crack in an infinite solid subjected to uniform stress.

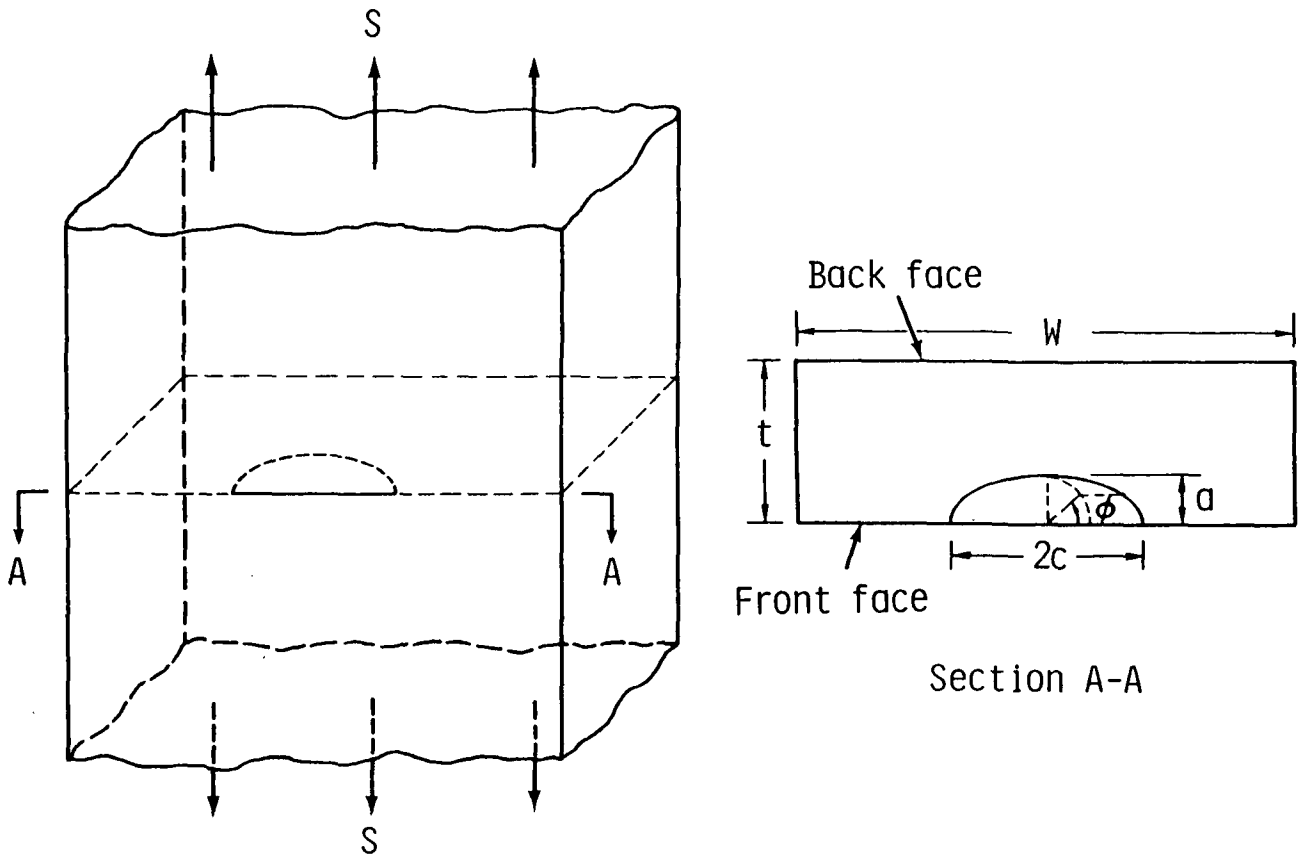

Fig. 2- Surface crack in a finite plate subjected to uniform stress.

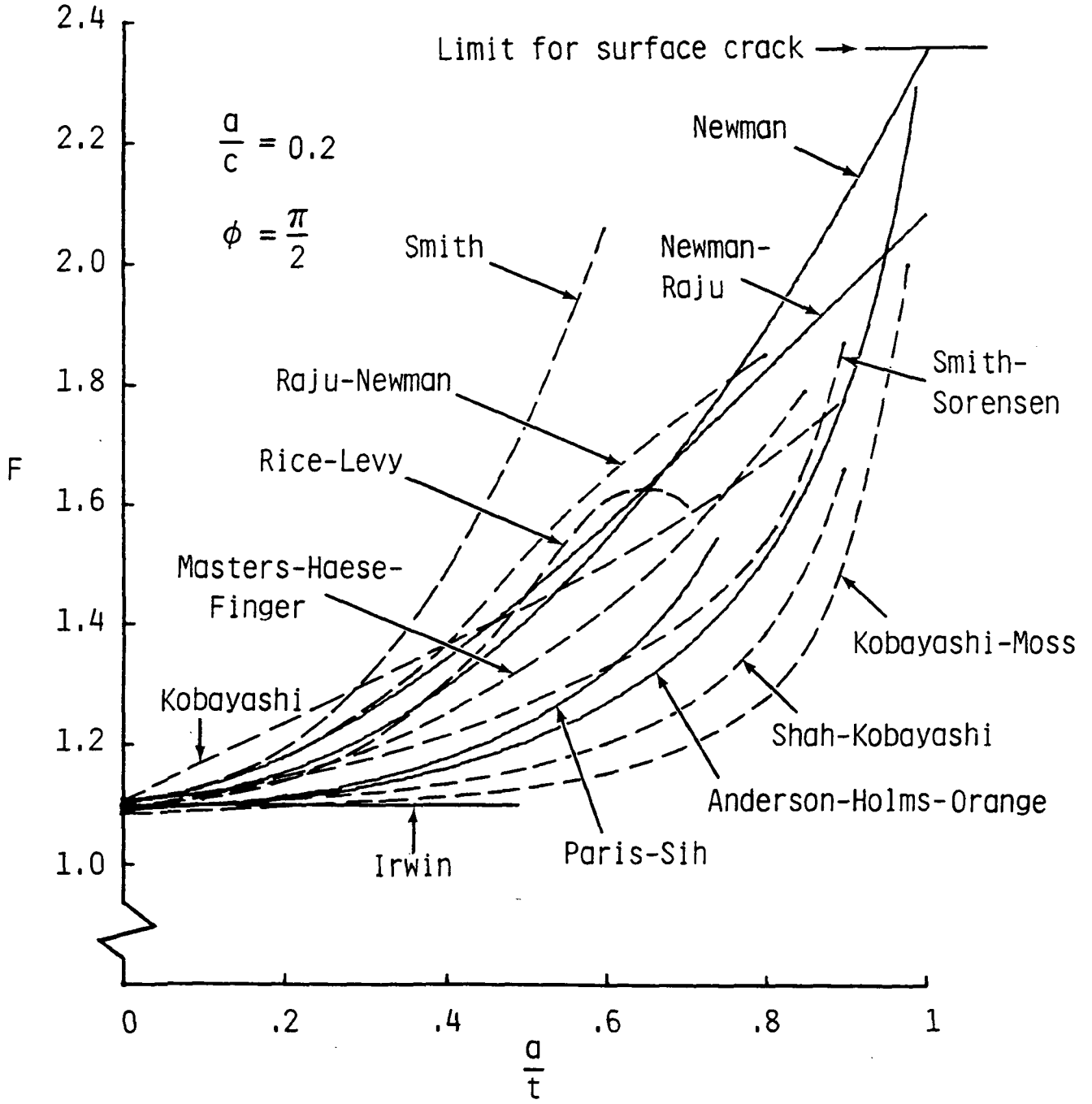

Fig. 3- Stress-intensity correction factor at maximum depth point for semi-elliptical surface crack (a/c = 0.2).

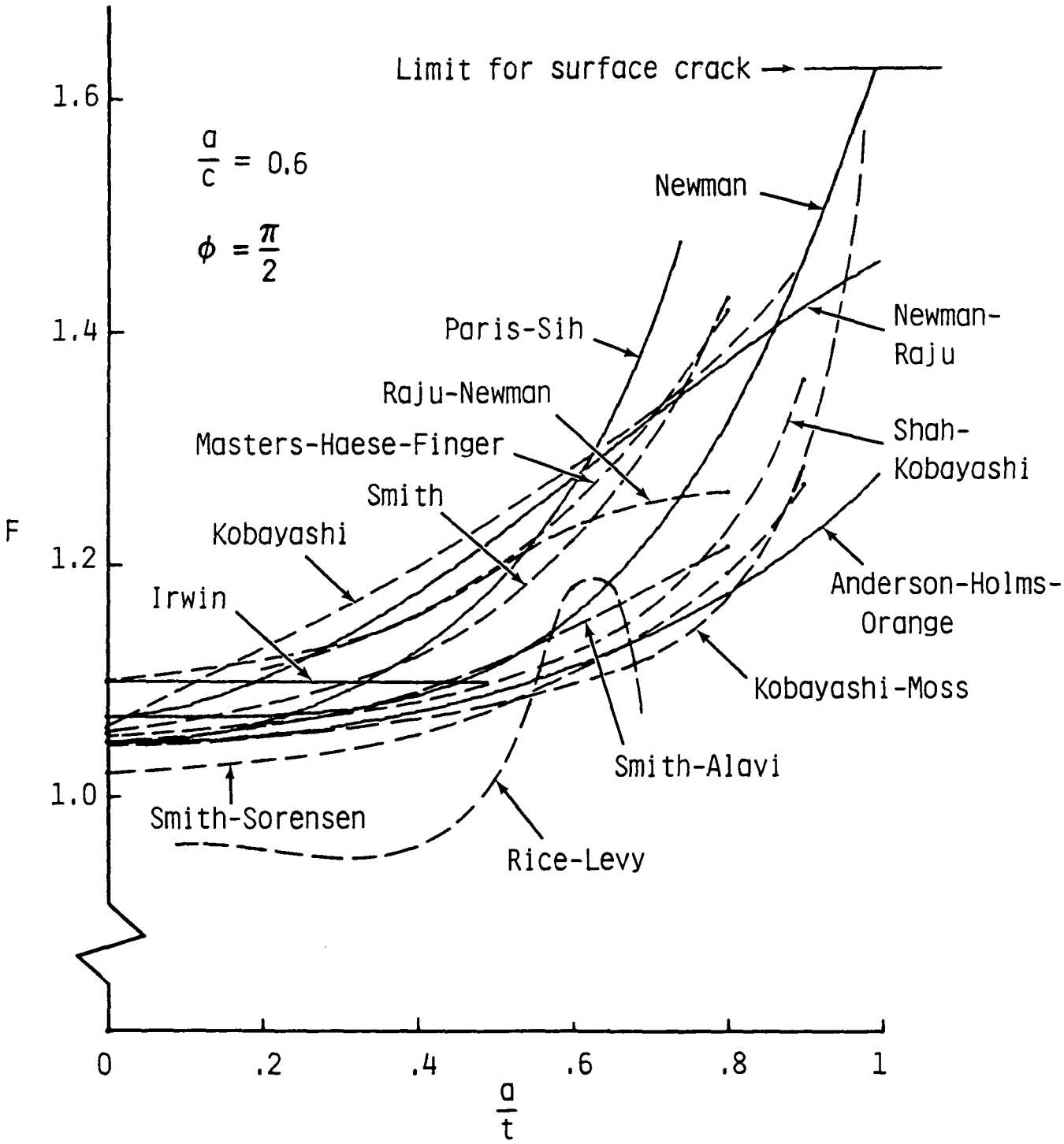

Fig. 4- Stress-intensity correction factor at maximum depth point for semi-elliptical surface crack (a/c = 0.6).

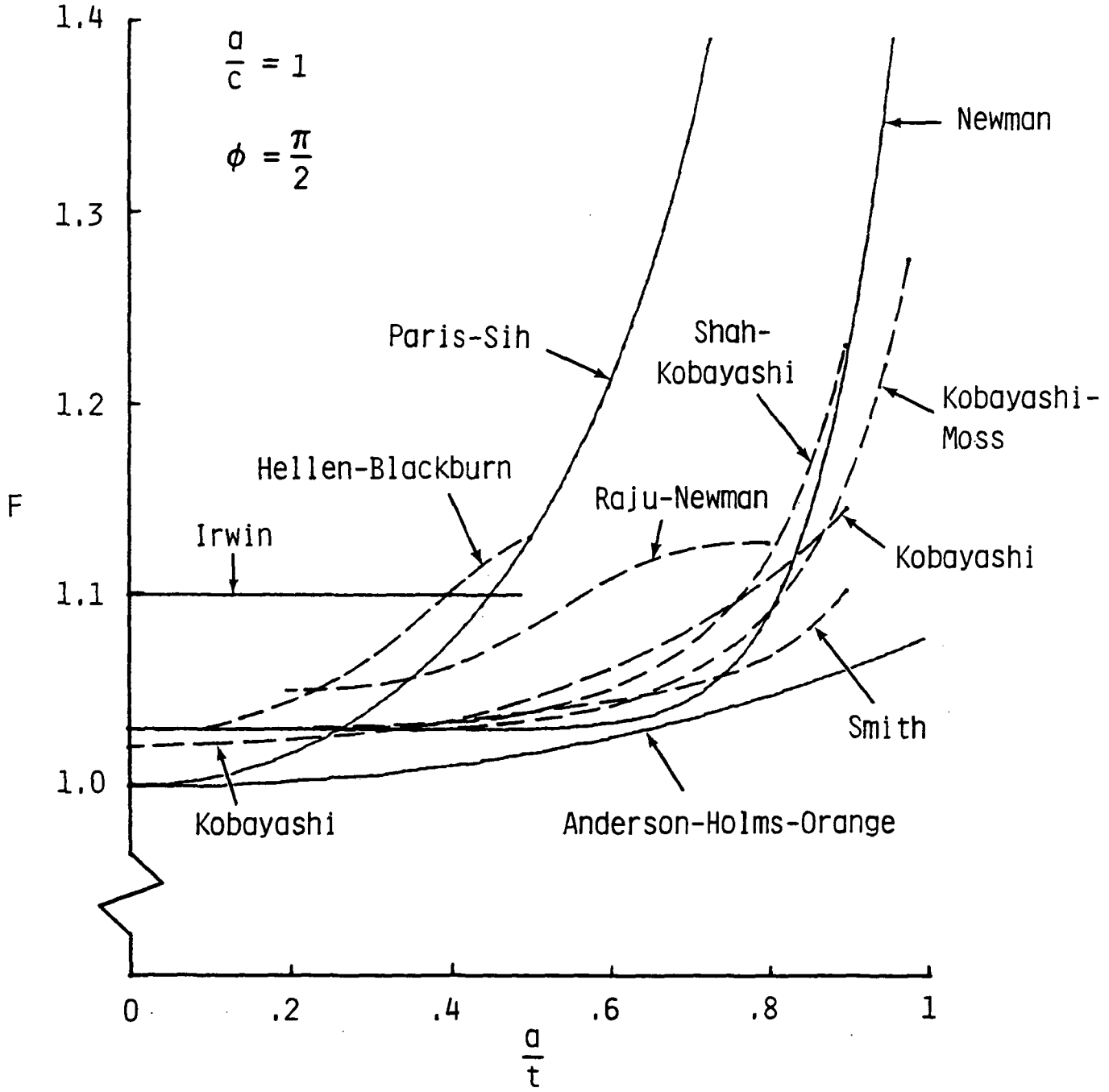

Fig. 5- Stress-intensity correction factor at maximum depth point for semi-circular surface crack (a/c = 1).

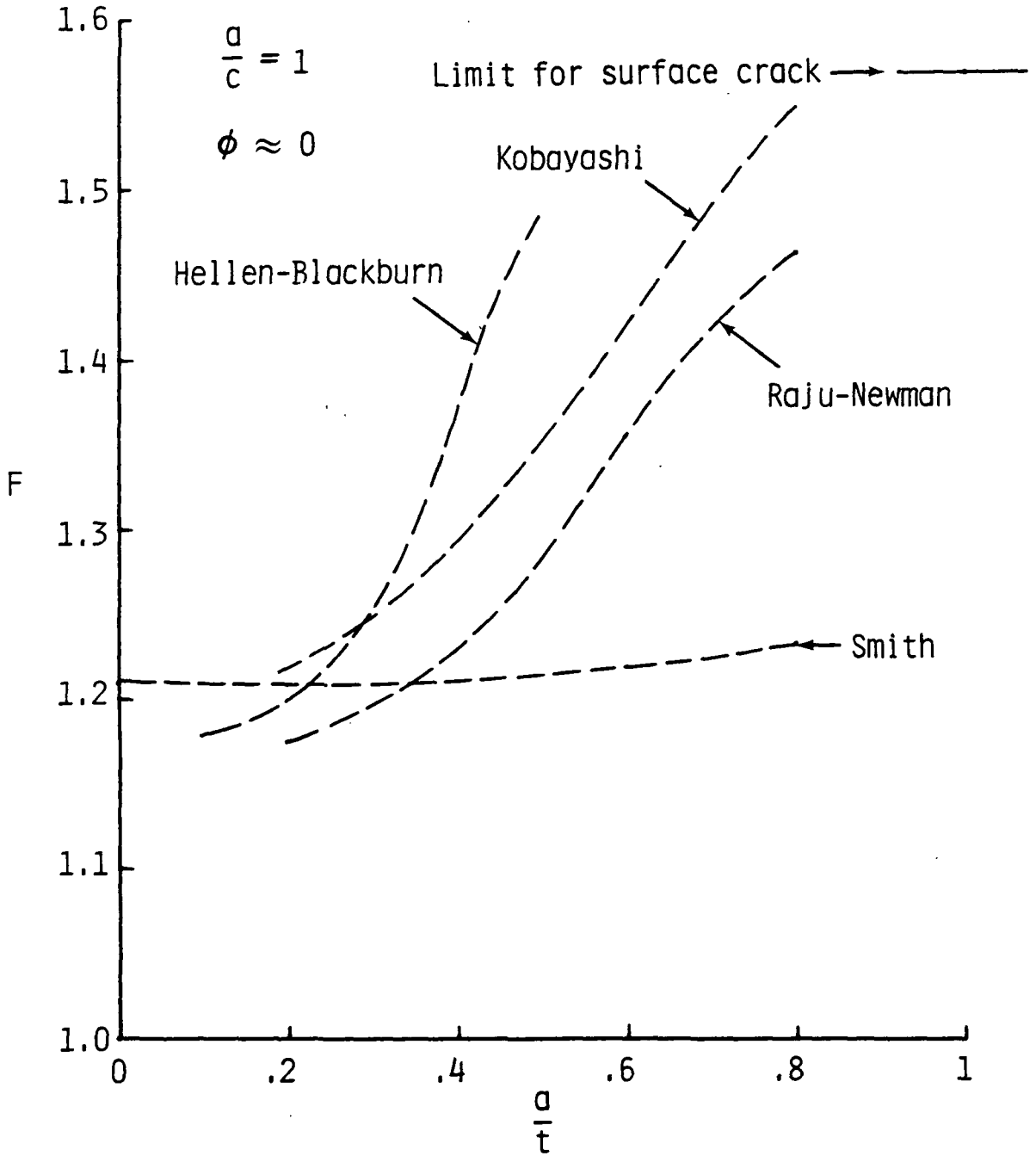

Fig. 6- Maximum stress-intensity correction factor for semi-circular surface crack (a/c = 1).

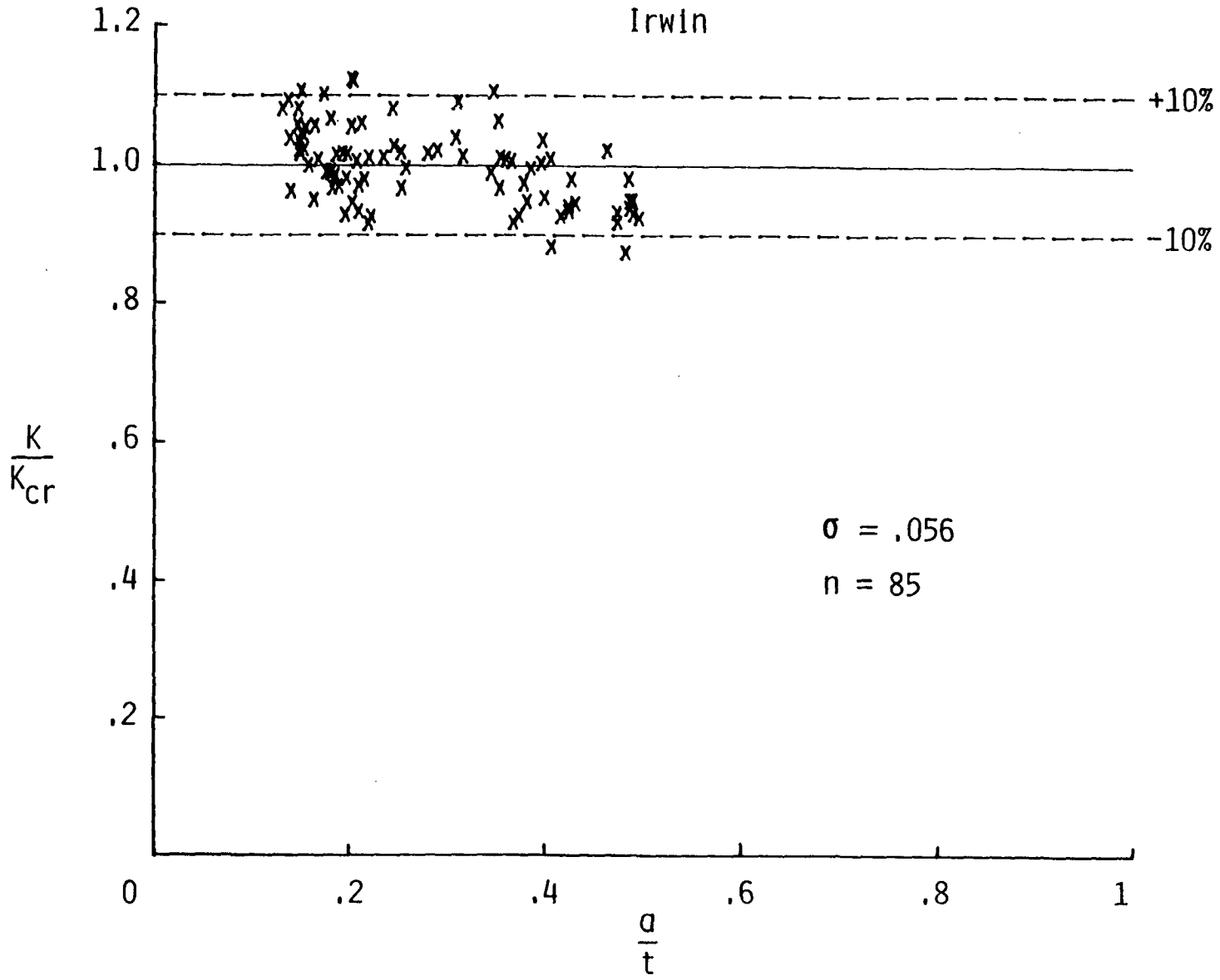

Fig. 7- Correlation of brittle-epoxy fracture data using the Irwin [1] solution.

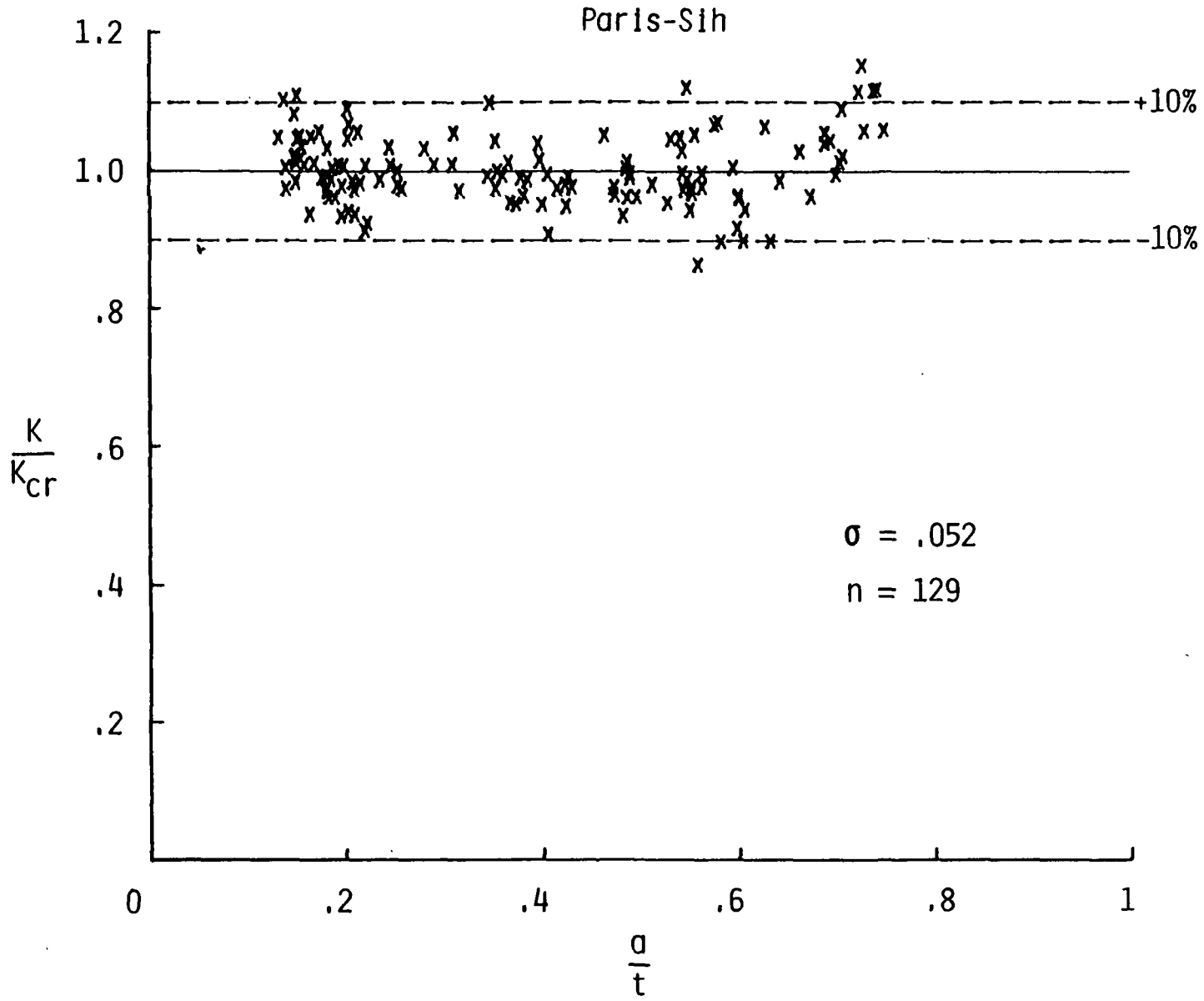

Fig. 8- Correlation of brittle-epoxy fracture data using the Paris-Sih [7] solution.

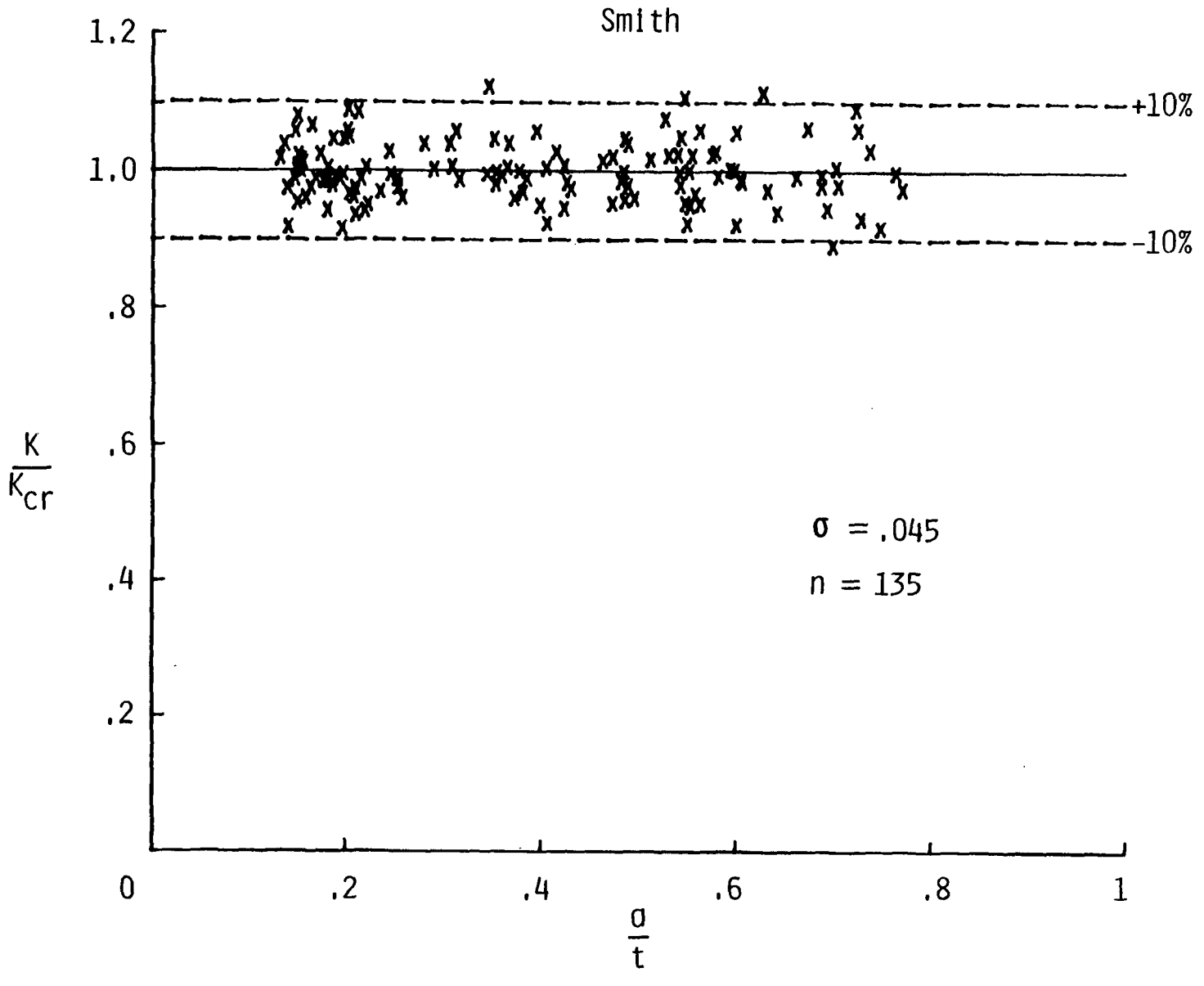

Fig. 9- Correlation of brittle-epoxy fracture data using the Smith [3,8] solution.

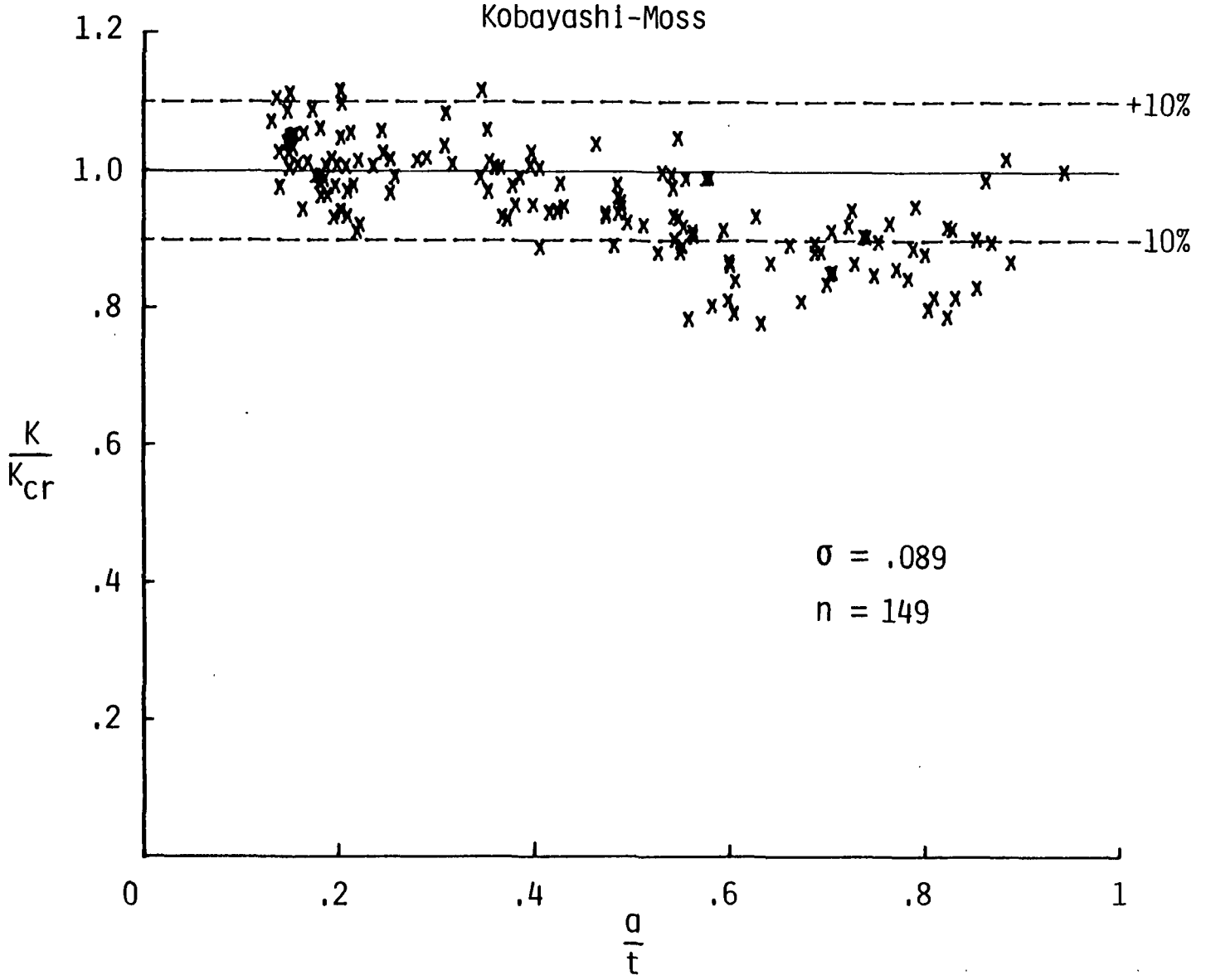

Fig. 10- Correlation of brittle-epoxy fracture data using the Kobayashi-Moss [10] solution.

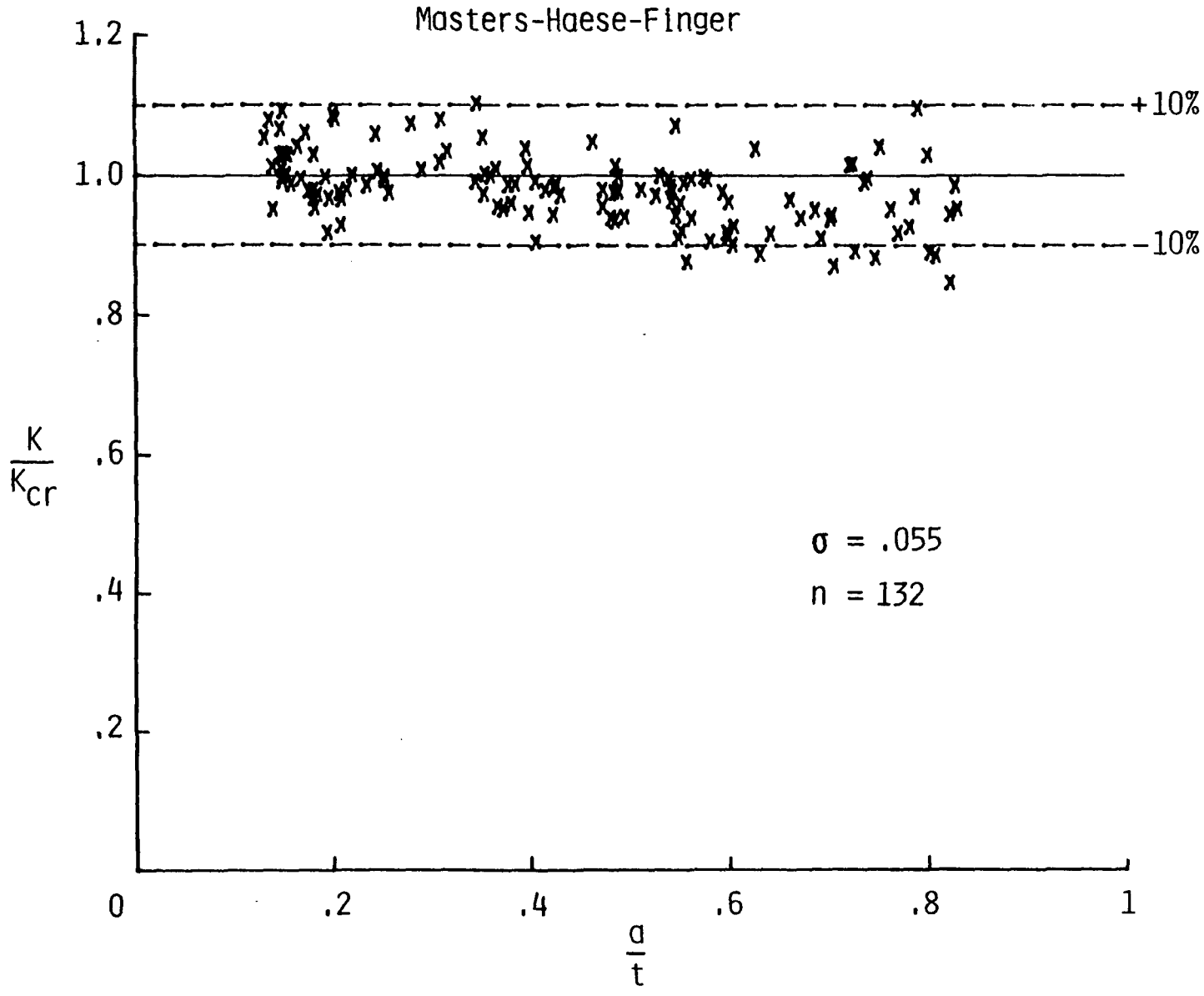

Fig. 11- Correlation of brittle-epoxy fracture data using the Masters-Haese-Finger [11] solution.

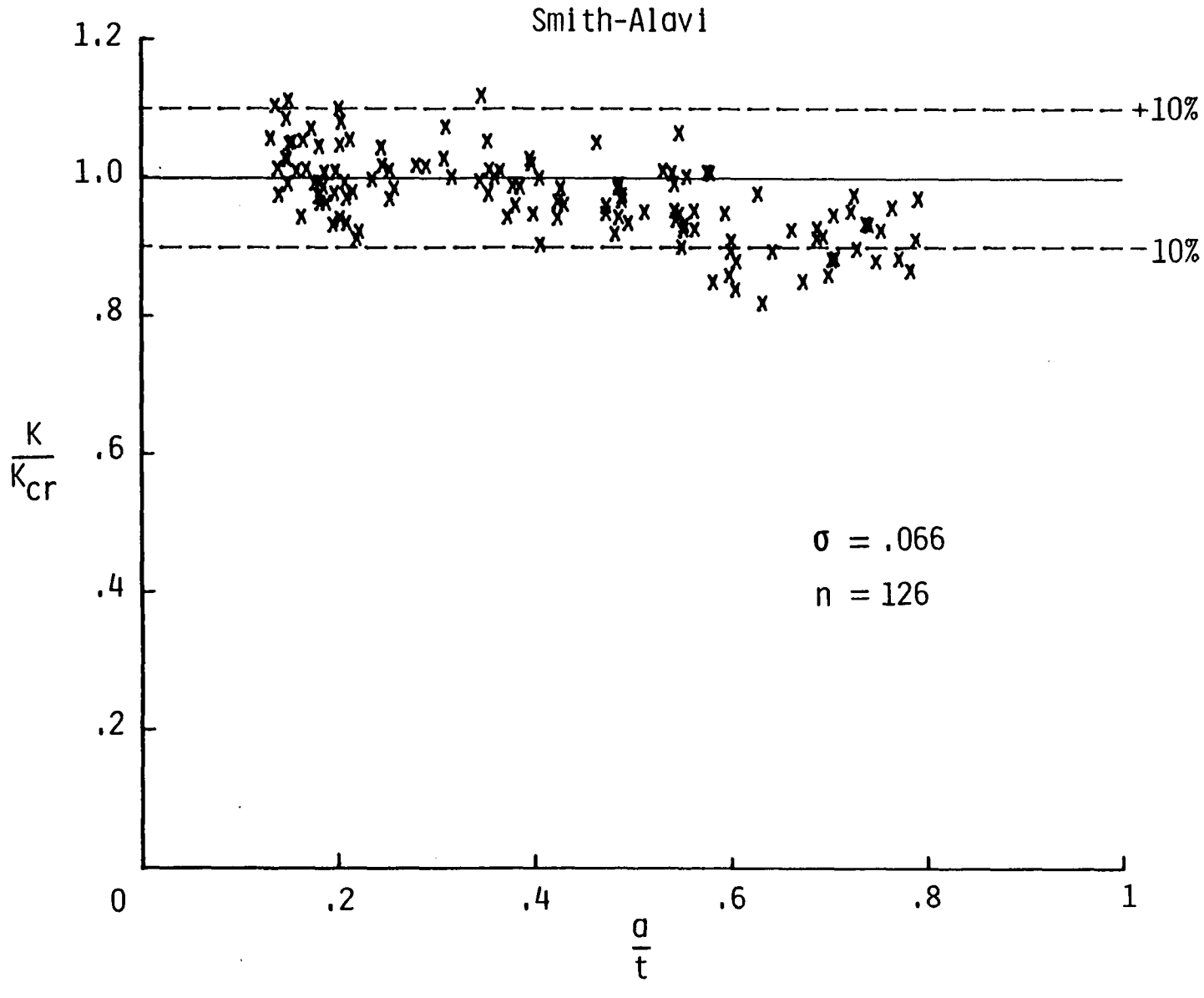

Fig. 12- Correlation of brittle-epoxy fracture data using the Smith-Alavi [13] solution.

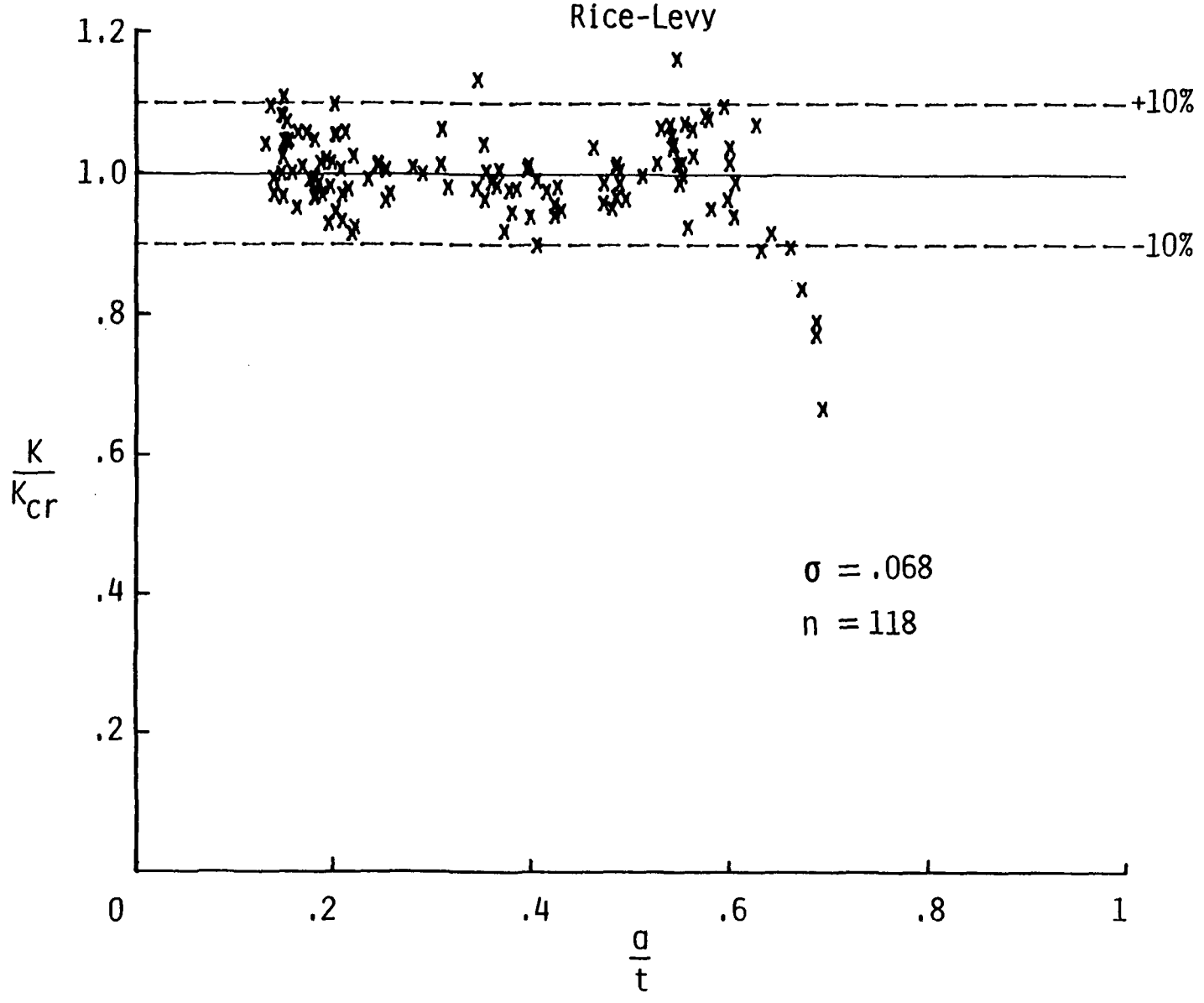

Fig. 13- Correlation of brittle-epoxy fracture data using the Rice-Levy [14] solution.

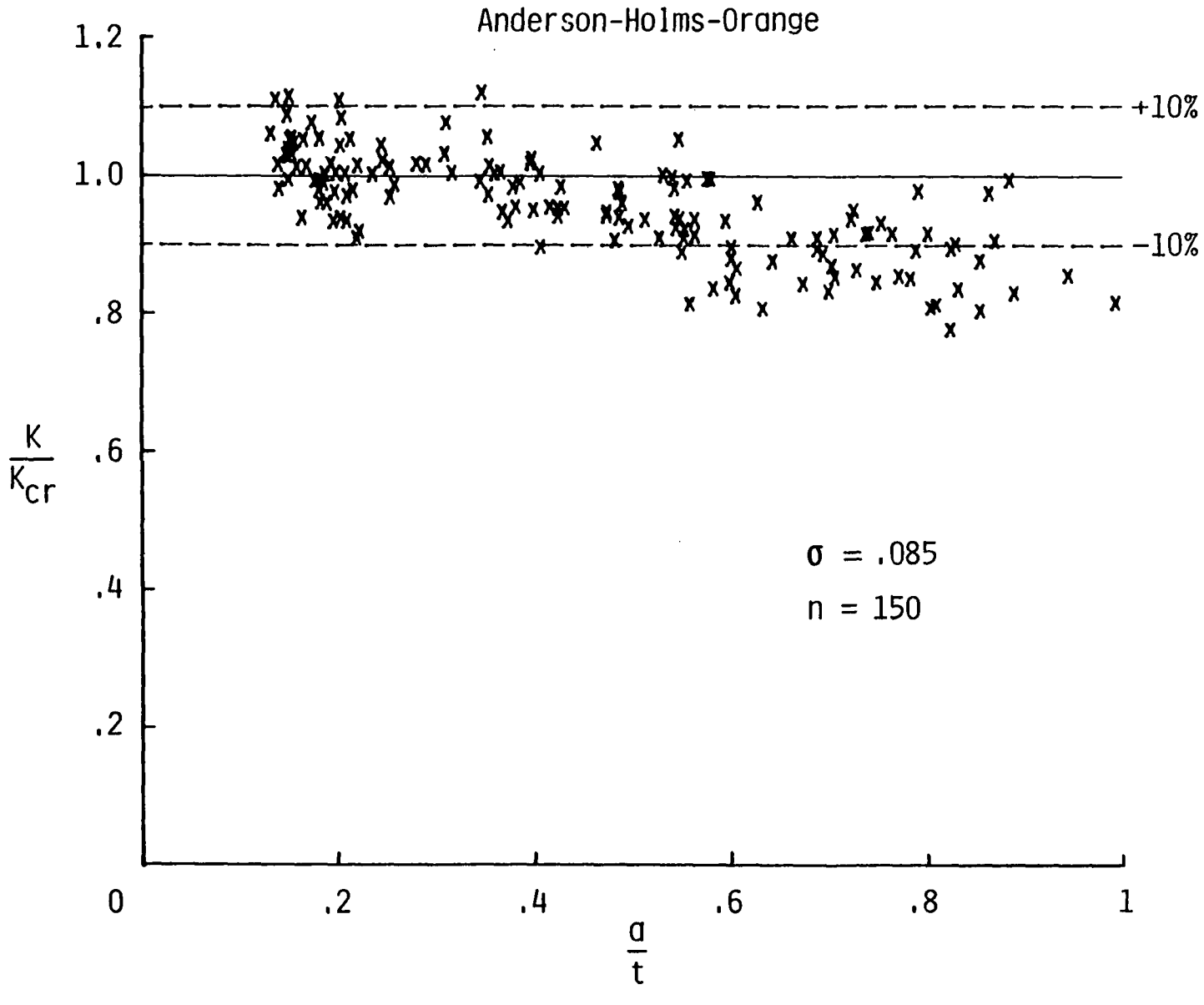

Fig. 14- Correlation of brittle-epoxy fracture data using the Anderson-Holms-Orange [15] solution.

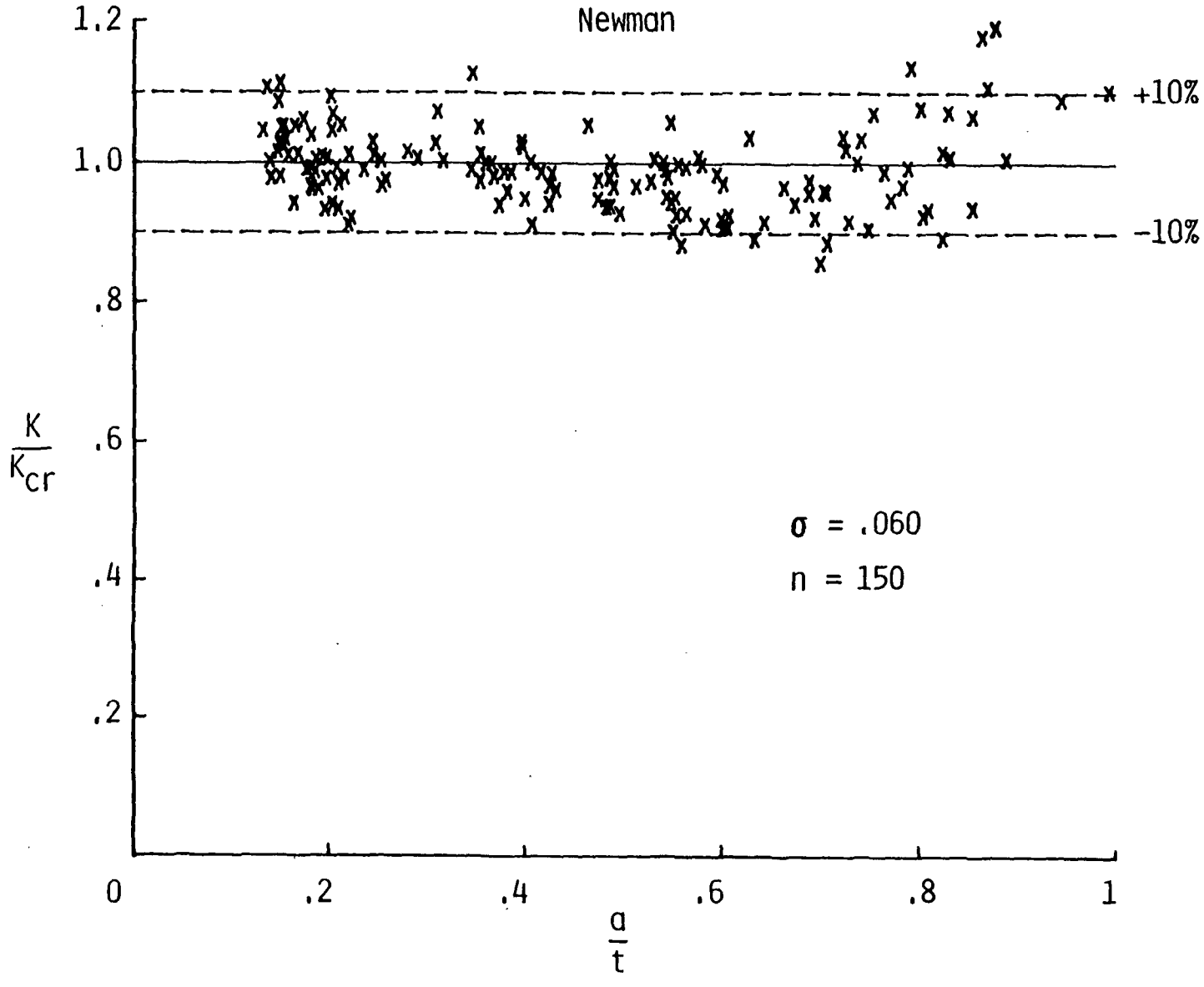

Fig. 15- Correlation of brittle-epoxy fracture data using the Newman [16] solution.

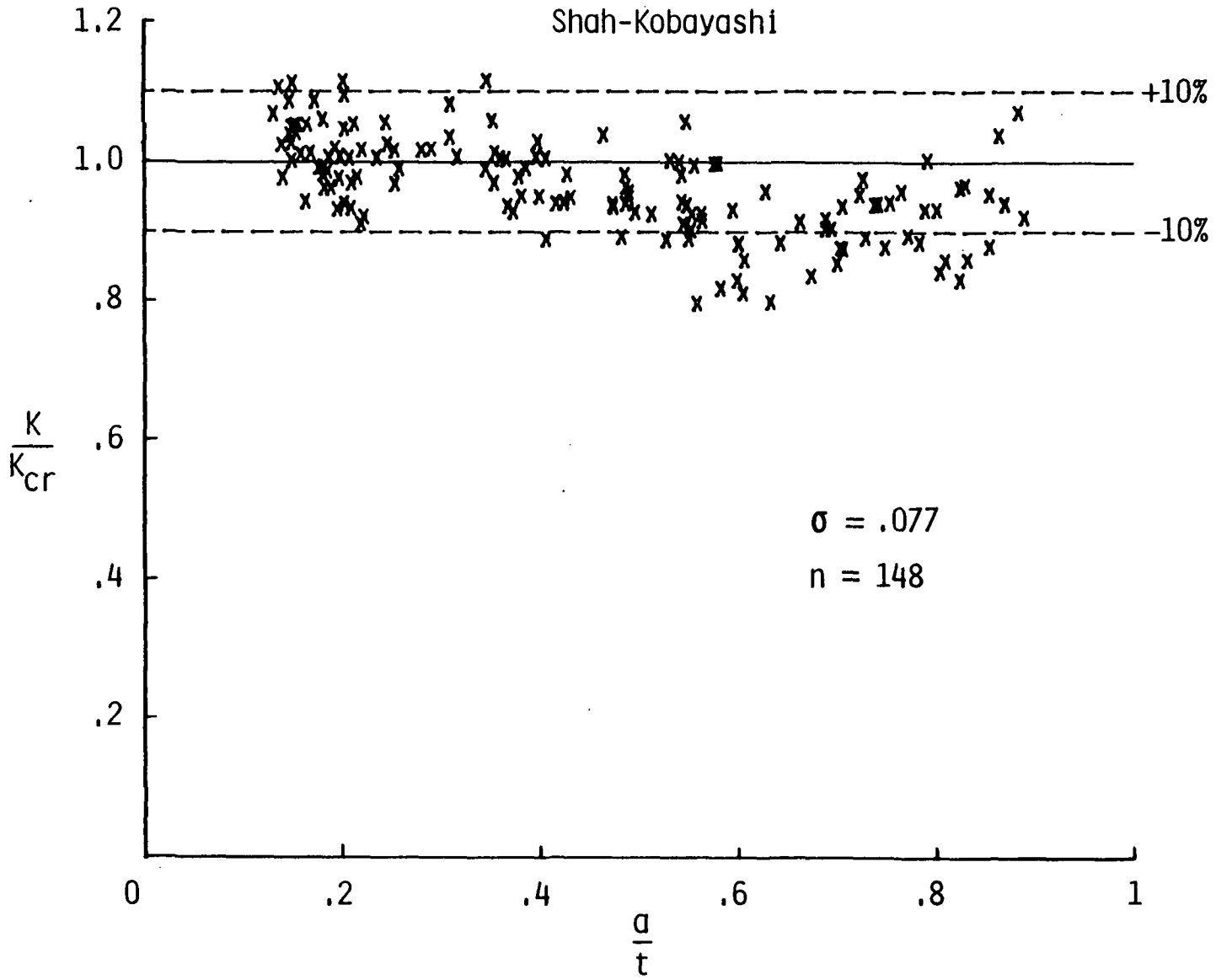

Fig. 16- Correlation of brittle-epoxy fracture data using the Shah-Kobayashi [17] solution.

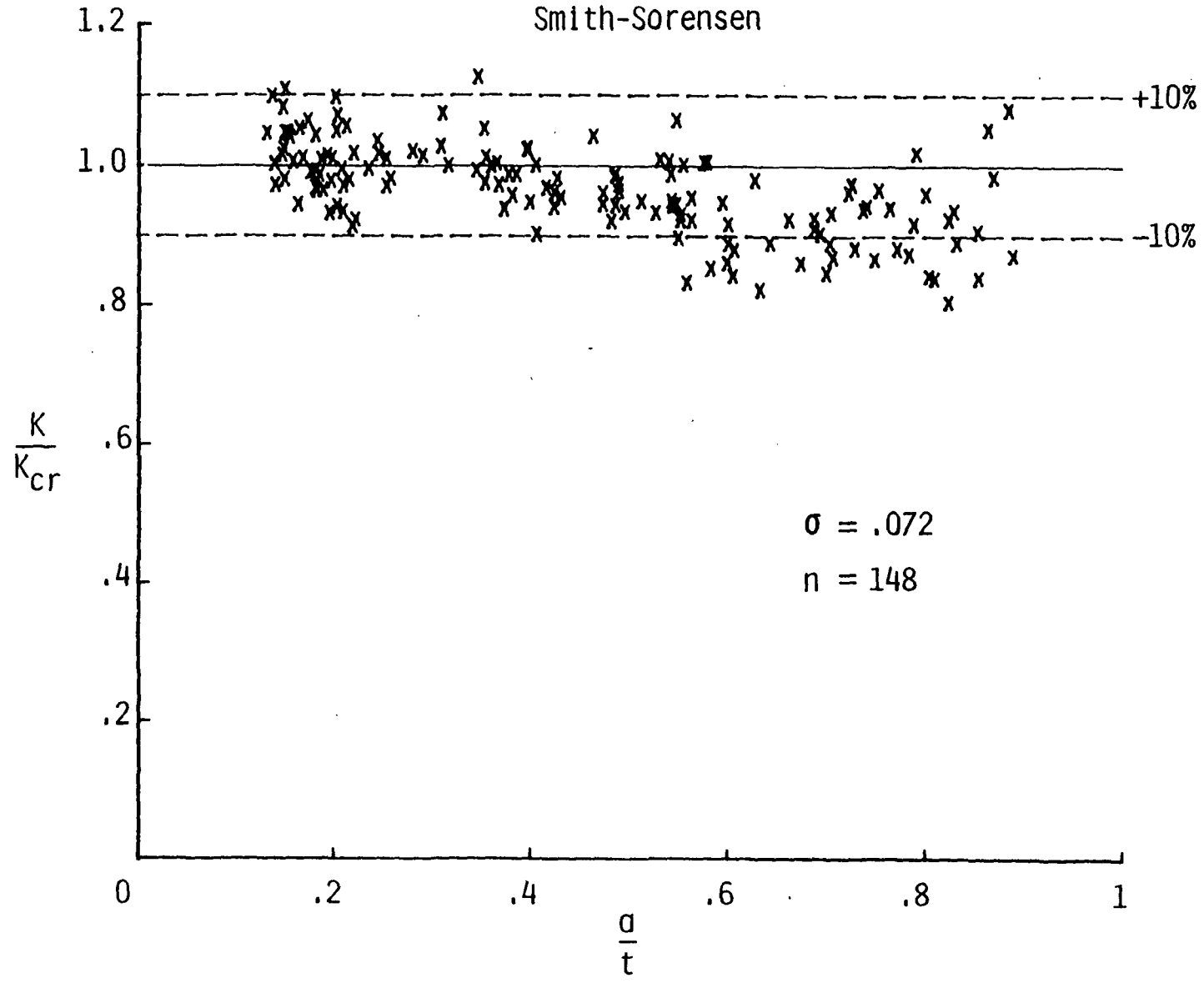

Fig. 17- Correlation of brittle-epoxy fracture data using the Smith-Sorensen [19] solution.

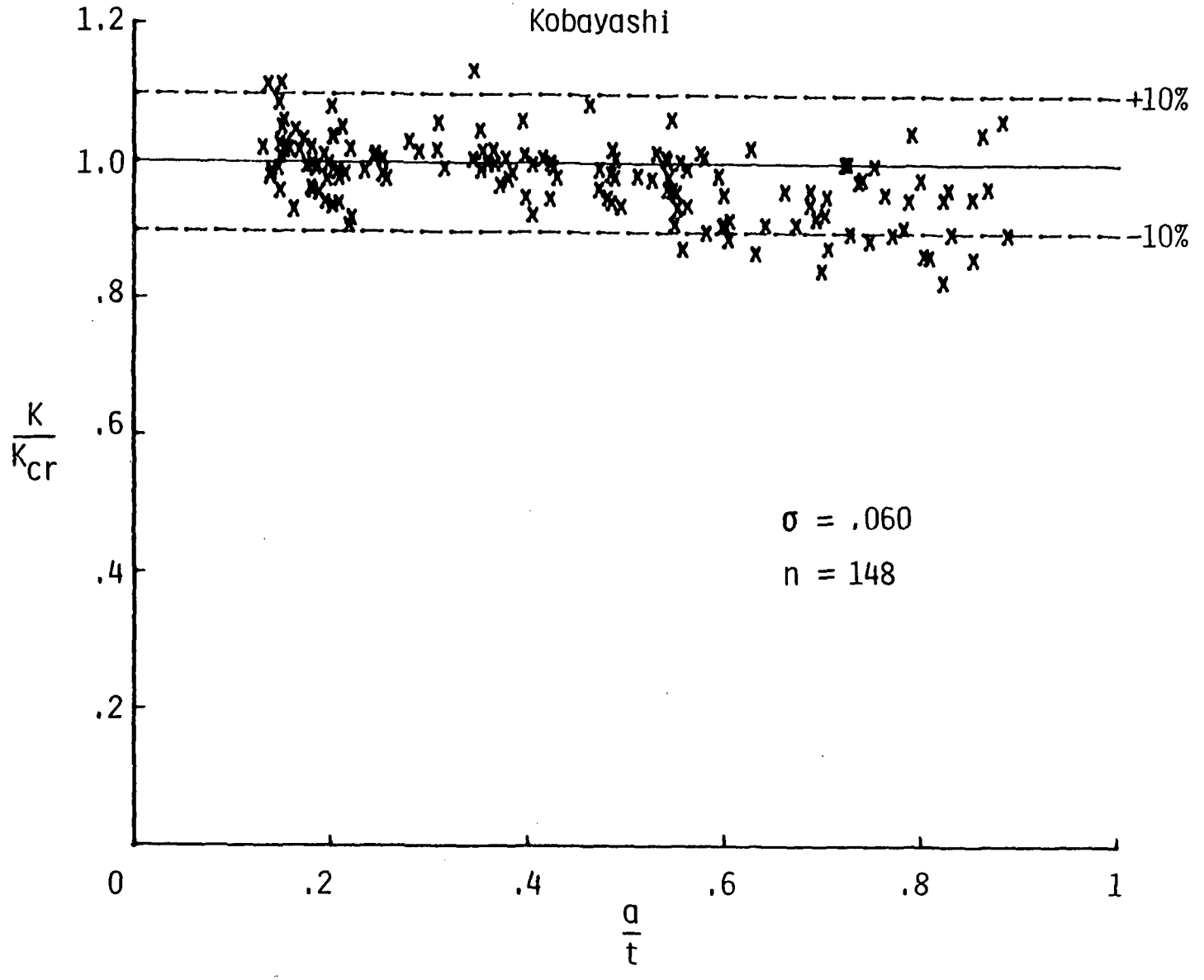

Fig. 18- Correlation of brittle-epoxy fracture data using the Kobayashi [20] solution.

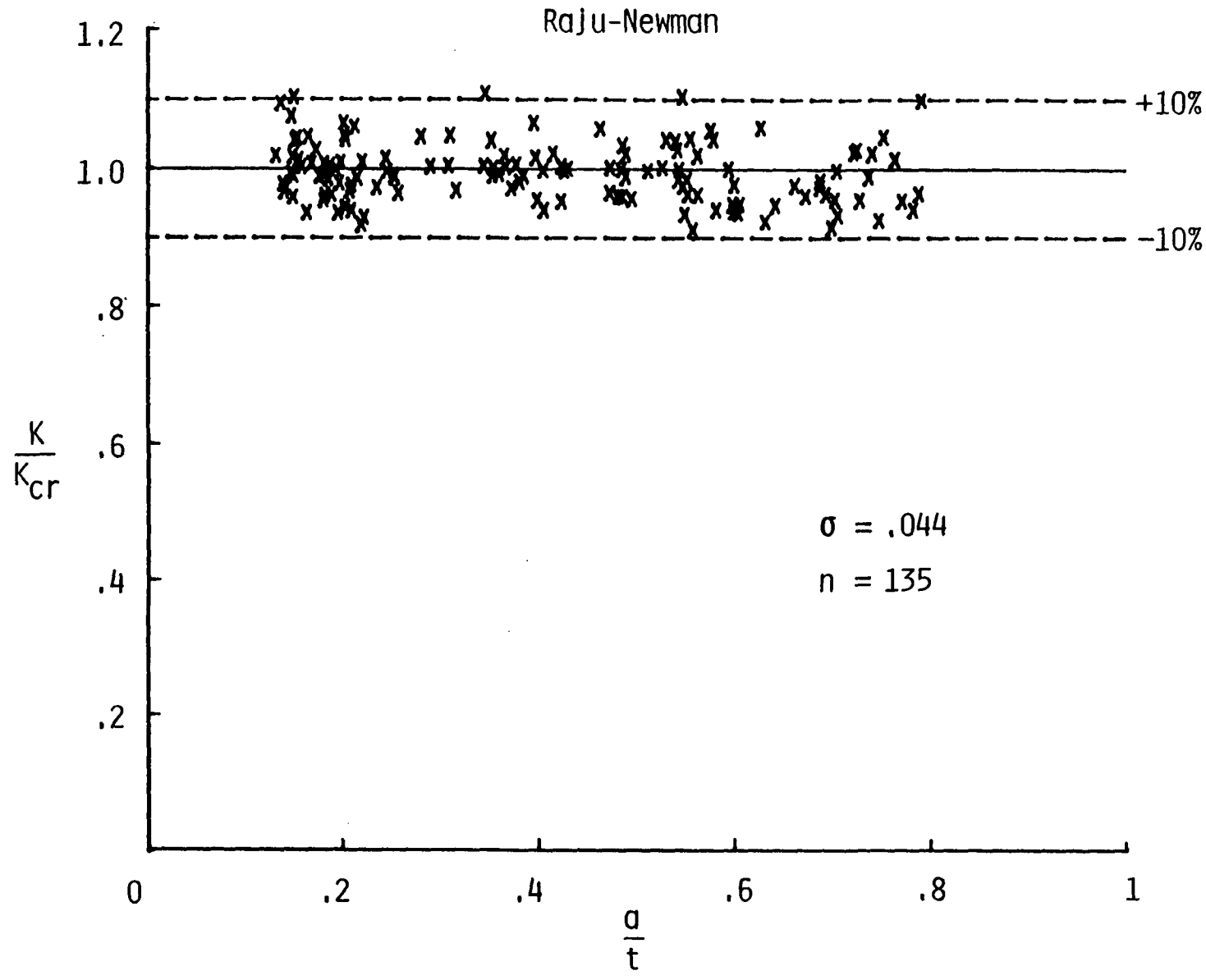

Fig. 19- Correlation of brittle-epoxy fracture data using the Raju-Newman [21,22] solution.

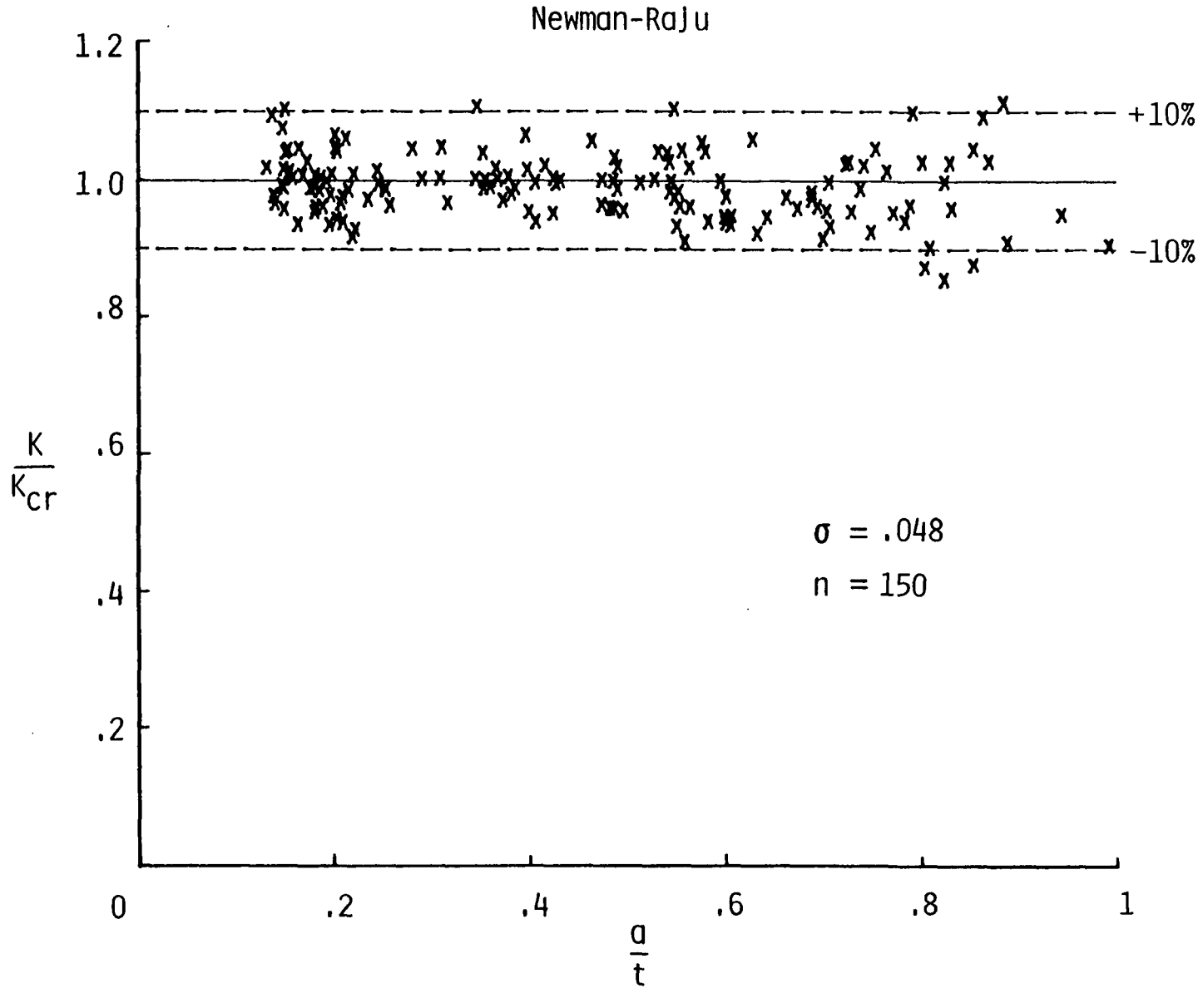

Fig. 20- Correlation of brittle-epoxy fracture data using the Newman-Raju (1978) solution.

1. Report No.	2. Government Accession No.	3. Recipient's Catalog No.
NASA TM-78805		

4. Title and Subtitle	5. Report Date
A REVIEW AND ASSESSMENT OF THE STRESS-INTENSITY FACTORS FOR SURFACE CRACKS	November 1978
	6. Performing Organization Code

7. Author(s)	8. Performing Organization Report No.
J. C. Newman, Jr.	

9. Performing Organization Name and Address	10. Work Unit No.
NASA Langley Research Center Hampton, VA 23665	506-17-23-03
	11. Contract or Grant No.
	13. Type of Report and Period Covered
12. Sponsoring Agency Name and Address	Technical Memorandum
National Aeronautics and Space Administration Washington, DC 20546	14. Sponsoring Agency Code

15. Supplementary Notes

Paper presented at the ASTM Symposium on Part-Through Crack Life Prediction, San Diego, CA, October 13-14, 1977.

16. Abstract

The stress-intensity factor solutions proposed for a surface crack in a finite plate subjected to uniform tension are reviewed. Fourteen different solutions for the stress-intensity factors are compared. These solutions have been obtained over the past 16 years using approximate analytical methods, experimental methods, and engineering estimates.

The present paper assesses the accuracy of the various solutions by correlating fracture data on surface-cracked tension specimens made of a brittle epoxy material. Fracture of the epoxy material was characterized by a constant value of stress-intensity factor at failure. Thus, the correctness of the various solutions are judged by the variations in the stress-intensity factors at failure. The solutions were ranked in order of minimum standard deviation. The highest ranking solutions correlated 95 percent of data analyzed within ±10 percent, whereas the lowest ranking solutions correlated 95 percent of data analyzed within ±20 percent. However, some solutions could be applied to all data considered, whereas others were limited with respect to crack shapes and crack sizes that could be analyzed.

17. Key Words (Suggested by Author(s))	18. Distribution Statement
Cracks Stresses Fracture properties Stress-intensity factors	Unclassified - Unlimited Subject Category 39

19. Security Classif. (of this report)	20. Security Classif. (of this page)	21. No. of Pages	22. Price*
Unclassified	Unclassified	49	$4.50

* For sale by the National Technical Information Service, Springfield, Virginia 22161

NASA-Langley, 1978